Sediment release of dissolved organic matter to the oxygen minimum zone off Peru

Alexandra N. Loginova[1], Andrew W. Dale[1], Frédéric A. C. Le Moigne[1,2], Sören Thomsen[1,3], Stefan Sommer[1], David Clemens[1], Klauss Wallmann[1], and Anja Engel[1]

[1]GEOMAR Helmholtz Centre for Ocean Research Kiel, Germany
[2]Mediterranean Institute of Oceanography, UM110, Aix Marselle Université, CNRS, IRD, 13288, Marselle, France
[3]LOCEAN-IPSL, IRD/CNRS/Sorbonnes Universites (UPMC)/MNHN, Paris, France

Correspondence: Anja Engel (aengel@geomar.de)

Abstract.

The eastern tropical South Pacific (ETSP) represents one of the most productive areas in the ocean that is characterised by a pronounced oxygen minimum zone (OMZ). Particulate organic matter (POM) that sinks out of the euphotic zone is supplied to the anoxic sediments and utilised by microbial communities. The degradation of POM is associated with dissolved

5   organic matter (DOM) production and reworking. The release of DOM to the overlying waters may represent an important organic matter escape mechanism from remineralisation within sediments but received little attention in OMZ regions so far. Here, we combine measurements of dissolved organic carbon (DOC) and dissolved organic nitrogen (DON) with DOM optical properties in the form of chromophoric (CDOM) and fluorescent (FDOM) DOM from porewaters and near-bottom waters of the ETSP off Peru. We evaluate diffusion-driven fluxes and net *in situ* fluxes of DOC and DON in order to investigate

10   processes affecting DOM cycling at the sediment-water interface along a transect 12°S. To our knowledge, these are the first data for sediment release of DON and porewater CDOM and FDOM for the ETSP off Peru. Porewater DOC accumulated with increasing sediment depth, suggesting an imbalance between DOM production and remineralisation within sediments. High DON accumulation resulted in very low porewater DOC/DON ratios (≤ 1) which could be caused by an "uncoupling" in DOC and DON remineralisation. Diffusion driven fluxes of DOC and DON exhibited high spatial variability. They varied

15   from 0.2 ± 0.1 mmol m^{-2}d^{-1} to 2.5 ± 1.3 mmol m^{-2}d^{-1} and from -0.04 ± 0.02 mmol m^{-2}d^{-1} to 3.3 ± 1.7 mmol m^{-2}d^{-1}, respectively. Generally low net *in situ* DOC and DON fluxes, as well as steepening of spectral inclination (*S*) of CDOM and accumulation of humic-like FDOM at the near-bottom waters over time indicated the active microbial DOM utilisation at the sediment-water interface. The latter may potentially be stimulated by nitrate (NO_3^-) and nitrite (NO_2^-) present in the water column. The microbial DOC utilisation rates, estimated in our study, may be sufficient to support denitrification rates of

20   0.2-1.4 mmol m^{-2}d^{-1}, suggesting that sediment release of DOM may on occasions contribute to nitrogen loss processes in the ETSP off Peru.

1 Introduction

The eastern tropical South Pacific (ETSP) is one of the most productive areas of the world ocean (Pennington et al., 2006). High productivity, followed by intensive organic matter remineralisation (e.g. Loginova et al., 2019; Maßmig et al., 2020) in combination with sluggish ventilation (Stramma et al., 2005; Keeling et al., 2010) leads to a formation of pronounced oxygen minimum zone (OMZ) (e.g. Stramma et al., 2008). Remineralisation of organic matter under anoxia induces nitrogen (N)-loss by denitrification, anammox as well as dissimilatory nitrate reduction to ammonium (DNRA) in the water column and sediments off the coast of Peru (Kalvelage et al., 2013; Arévalo-Martínez et al., 2015; Dale et al., 2016; Sommer et al., 2016; Glock et al., 2019). Although organic matter remineralisation is classically assumed to be limited by the absence of oxygen (Demaison and Moore, 1980), recent studies report similar abilities of marine microbes to degrade organic matter in oxygenated surface waters and within OMZs (Pantoja et al., 2009; Maßmig et al., 2019, 2020), suggesting that other factors, such as the quality of organic matter may regulate microbial activity within OMZs (Pantoja et al., 2009; Le Moigne et al., 2017). Similar to the water column studies, extensive fieldwork campaigns conducted on sediments off Peru also suggested intensive particulate organic matter (POM) remineralisation under full anoxia (Dale et al., 2015).

While POM degradation in sediments is mostly associated with its full remineralisation to dissolved inorganic carbon (DIC) and inorganic nutrients, the mechanism of POM remineralisation implies important intermediate stages of dissolved organic matter (DOM) production, reworking and mineralisation (Smith et al., 1992; Komada et al., 2013). Thus, around 10 % of remineralised particulate organic carbon (POC) may accumulate as dissolved organic carbon (DOC) in the porewaters (Alperin et al., 1999). In turn, DOM efflux may represent an important escape mechanism for carbon from sediments (e.g. Ludwig et al., 1996; Burdige et al., 1999) and a source of organic matter to the water column (e.g. Burdige et al., 2016). Despite the acknowledged importance of sediment DOM for organic matter cycling, the measurements of benthic DOM fluxes remain scarce, and the reactivity of the porewater DOM is not well constrained.

The release of dissolved substances from anoxic sediments is regulated mainly by diffusion through the sediment-water interface (e.g. Lavery et al., 2001, and references therein). Diffusion-driven DOM fluxes (hereafter named "diffusive fluxes") and net DOM fluxes (hereafter termed "*in situ* net fluxes") are commonly evaluated from porewater gradients using Fick's First Law and by enclosing and incubating a small area of the sediment surface over time, respectively. Diffusive DOM fluxes are, generally, consistent with net DOM fluxes in non-bioturbated anoxic sediments (Burdige et al., 1992). In some sediments, however, the diffusive flux may overestimate the net flux (Burdige et al., 1992; Lavery et al., 2001). This overestimation may be attributed to bioturbation, "unfavourable" redox conditions (Lavery et al., 2001), irreversible adsorption onto particles, and biological DOM consumption at the sediment-water interface or in the bottom waters (Burdige et al., 1992). The determination of *in situ* net DOM fluxes using benthic incubation chambers are independent of such uncertainties. This approach is based on the assumption that solutes, released into the benthic chamber, behave conservatively during the timecourse of the incubation, and, show linear trends over time.

It was suggested previously that porewater DOM consists of recalcitrant low molecular weight (LMW) compounds (Burdige and Gardner, 1998; Burdige and Komada, 2015). Therefore, the sediment outflux of DOM was hypothesised to serve as an

important source of recalcitrant DOM to the water column (e.g. Burdige and Komada, 2015; Burdige et al., 2016). On the other hand, elevated concentrations of dissolved organic nitrogen (DON) suggest the presence of labile proteinaceous organic matter in the porewaters (e.g. Faganeli and Herndl, 1991). Furthermore, measurements and modelling of isotopic carbon composition in the anoxic and suboxic sediments off California, suggest that about 50 % of DOM within upper sediments represents isotopically young and labile DOM components, that may be released to the water column, where they are actively utilised by heterotrophs (Bauer et al., 1995; Komada et al., 2013; Burdige et al., 2016).

Similarly to DOM in the water column, porewater DOM consists of a complex mixture of organic components, only a little fraction of which may be characterised by chemical analyses (e.g. Burdige and Komada, 2015). Therefore, examining the elemental composition of DOM or its optical properties may be useful for accessing quality and reactivity of porewater DOM. The elemental ratio (DOC/DON) that is commonly used for inferring organic matter bioavailability in the water column, in sediment porewaters, displays controversial patterns. Some of the studies suggest that low DOC/DON ratios of 2 to 5 found in sediments with reduced O_2 levels, may indicate an accumulation of bioavailable DOM under low O_2 conditions (Faganeli and Herndl, 1991; Alkhatib et al., 2013). On the other hand DOC/DON ratios found in other studies were lower under oxygenated conditions compared to those of anoxic sediments (Burdige and Gardner, 1998).

Optical properties were also shown to provide important insights in DOM cycling not only in the water column (e.g. Coble, 1996; Zsolnay et al., 1999; Jørgensen et al., 2011; Catalá et al., 2016; Loginova et al., 2016) but also in porewaters of marine and freshwater sediments (e.g. Chen et al., 2016). The fraction of DOM that exhibits optical activity owing to the presence of chromophoric groups — a combination of conjugated double bonds and heteroatoms — in its molecular structure is referred to as chromophoric DOM (CDOM) and fluorescent DOM (FDOM). CDOM refers to DOM that absorbs light over a broad spectrum from UV to visible wavelengths. A typical CDOM absorbance spectrum is shaped as an exponential curve (Del Vecchio and Blough, 2004). The spectral inclination (S) and absorption coefficients are used to learn on bulk DOM properties. For instance, steepness of S is suggestive of relative differences in DOM molecular weight. Thus, a decrease of CDOM absorption in the visible spectra, compared to UV wavelength implies a decrease in DOM molecular weight (e.g. Helms et al., 2008). Those changes in the optical properties occur due to the ability of high molecular weight (HMW) DOM to absorb light at longer wavelengths, compared to LMWDOM. The part of CDOM is fluorescent due to its aromatic nature is referred to as FDOM and is used to infer DOM quality (Coble, 1996; Zsolnay et al., 1999; Jørgensen et al., 2011; Catalá et al., 2016; Loginova et al., 2016). Thus, 3D fluorescence spectroscopy, followed by parallel factor analysis (PARAFAC), has been recognised as a useful tool for distinguishing between different organic matter pools (Murphy et al., 2013). Fluorophores that are excited and emit at UV wavelengths are often referred to as amino acid-like DOM. Components that are excited at UV, but emit at visible wavelengths, are mainly referred to as humic-like or fulvic-like DOM (e.g. Coble, 1996; Murphy et al., 2014, and references therein). Thus, based on optical measurements, similar suggestions as in studies based on isotopic and elemental DOM composition could be drawn. For instance, CDOM distributions in sediment cores from the Chukchi Sea suggested that anoxic sediments may serve as a production site of humic-like substances and a potential source of pre-altered DOM into the water column (Chen et al., 2016). In turn, FDOM measurements made during incubations of sediment cores (Yang et al., 2014), indicated that DOM released into the overlying water might also be further altered by microbial communities, serving as a source of bioavailable

organic matter. In the ETSP off Peru, fine-scale spatial resolution FDOM measurements suggested DOM release from anoxic sediments into the water column (Loginova et al., 2016). High FDOM fluorescence associated with the benthic release of DOM reached the euphotic zone, likely influencing organic carbon turnover of the whole water column. Hence, sediment release of DOM could potentially serve as an important carbon and N source (e.g. Moran and Zepp, 1997) and reduce penetration depth

5 of light in the water column (e.g. Belzile et al., 2002) for pelagic microbial communities, affecting biogeochemical processes of the water column. However, the release of porewater DOM and its reactivity had not been well studied yet in the area. In this study, we combine measurements of diffusive and in situ net fluxes of DOC and DON and interpret those fluxes in relation to DOM optical properties measured in the sediments in the Peruvian OMZ. Our objectives are to provide a deeper understanding of DOM cycling in Peruvian sediments.

10 ## 2 METHODS

2.1 Study area

Sediment sampling was carried out in April-May 2017 during research cruises M136 and M137 to the Peruvian OMZ on board of RV Meteor. The sampling area was located between 12-12.2 °S and 77.1-77.3 °W (Fig. 1). In total, six stations (see Table 1) were sampled along the transect 12°S (12°S) on the middle shelf, outer shelf and continental slope (Dale et al., 2015, 2016;

15 Sommer et al., 2016).

During the study, the water column at the sampling stations was subjected to a consistent poleward flow ranging from 0.1 to $0.5 \, \mathrm{m \, s^{-1}}$ (Lüdke et al., 2019). Low-oxygen ($\ll 5 \, \mathrm{\mu mol \, kg^{-1}}$) waters were observed above the sediment, with the exception for station 2 (St.2), where the O_2 concentration was slightly above $10 \, \mathrm{\mu mol \, kg^{-1}}$. This may have been a remnant of the coastal el Niño that occurred 3–4 months prior to our fieldwork (Rodríguez-Morata et al., 2019) or intensification of poleward flow,

20 observed in May 2017 (Lüdke et al., 2019). The highest concentrations of water column nitrate (NO_3^-) and nitrite (NO_2^-) were observed at stations $\geq 100 \, \mathrm{m}$ depth, while at shallower stations ammonium (NH_4^+) concentrations up to $1.2–1.4 \, \mathrm{\mu mol \, L^{-1}}$ were detected (Lüdke et al., 2019).

Sediments at the sampling stations are fine-grained diatomaceous dark-olive anoxic muds (Gutiérrez et al., 2009; Mosch et al., 2012) with porosity ranging between 0.8 and >0.9 (Table 1). In previous studies, polychaetes and oligochaetes were

25 found in the sampling area (Dale et al., 2015; Sommer et al., 2016). However, the sediment showed little evidence of strong mixing by bioturbation (Bohlen et al., 2011; Dale et al., 2015). In turn, the sediments were densely colonised by mats of large filamentous sulphur bacteria of the genera *Thioploca* and *Beggiatoa* (Gutiérrez et al., 2009; Mosch et al., 2012). Dale et al. (2015) reported that mats of these sulphide oxidising bacteria cover up to 100 % of the sediment surface at shallowest stations extending their trichomes 2 cm into the water column to access bottom water NO_3^-. They could be observed from the sediment

30 surface down to 20 cm sediment depth. At offshore stations, bacterial mats of several dm in diameter were covering up to 40 % of the sediment surface. Their occurrence was related to high carbon rain rates, which ranged from $10 \, \mathrm{mmol \, m^{-2} d^{-1}}$ on the continental slope to $80 \, \mathrm{mmol \, m^{-2} d^{-1}}$ on the shallowest shelf station (Fig.S1). Furthermore, the region was characterised by substantial organic matter utilisation as indicated from high DIC fluxes and porewater NH_4^+ concentrations (Dale et al., 2015).

Thus, despite the highest sediment accumulation rates and POC content of the sediments, the highest organic matter respiration, as follows from large sediment DIC (Dale et al., 2015) and NH_4^+ (Sommer et al., 2016) fluxes at middle shelf stations, led to the smallest percentage of carbon burial efficiency ($\sim$17%), compared to the outer shelf and the continental slope (24-74 %) (Fig.S1). Furthermore, Sommer et al. (2016) and Dale et al. (2015) suggested spatial variability of biological N cycling pathways in the area. Thus, outer shelf stations displayed the highest sediment uptake rate of NO_3^- and NO_2^- followed by high N_2 outflux (Sommer et al., 2016). At shallower stations, NO_3^- and NO_2^- were entirely exhausted and excessively high fluxes of NH_4^+ were observed (Fig.S1). Those spatial variabilities in N fluxes were suggested to be a result of dominating mechanisms of denitrification and anammox on the outer shelf and continental slope, and DNRA in the middle shelf. A further detailed description of the sediment and bottom waters at 12°S may be found in Dale et al. (2015, 2016) and Sommer et al. (2016).

2.2 Field sampling and sample preparation

Two benthic landers (Biogeochemical Observatory (BIGO) I and II) (Sommer et al., 2008) were deployed (see Table 1). Both were equipped with two circular flux chambers with an internal diameter of 28.8 cm. Volumes of the bottom water enclosed in the benthic chambers varied from $\sim$12 to $\sim$20 L during the study. Each BIGO chamber was equipped with eight glass syringes, which were filled sequentially to determine the net *in situ* flux of solutes across the sediment-water interface (Fig. S2). A detailed description of the BIGO lander can be found in Sommer et al. (2008) and Dale et al. (2014).

At each station, water from one BIGO chamber (chamber 2) was used for the DOM sampling. Samples for DOC, DON and CDOM and FDOM analyses were taken at $\sim$0.2, 4, 9, 12, 17, 21, 25 and 30 hrs after the beginning of sediment incubation.

All samples were passed through pre-washed (60 mL of ultrapure water) cellulose acetate (CA) membrane syringe filters (0.2 µm) and first five mL of the filtrate was discarded to waste before filling the sample into storage vials. Several types of filters (PES, nylon, CA and regenerated cellulose (RC)) were examined for background DOC and total dissolved nitrogen (TDN) signal before the cruise. CA and RC filters gave minimal background concentrations for both parameters after rinsing with 60 ml of ultrapure water (Fig.S4). CA filters were chosen over RC due to their lower binding affinity to macromolecules and proteins.

Filtered samples were filled into pre-combusted (450°C, 8 hrs) amber glass vials for CDOM and FDOM and into pre-combusted (450°C, 8 hrs) clear glass ampoules for DOC and DON analyses. The latter samples were fixed with 20 µl of ultra-pure HCl (30 %: Merck Chemicals GmbH) and flame sealed before storage. All samples were stored (1-2 month) at +4 °C in the dark pending analysis in the home laboratory.

The porewater DOM distribution and properties, as well as diffusive fluxes, were quantified by analysing DOC, DON, CDOM and FDOM in sediment cores obtained using multiple corers (MUCs). Retrieved sediments were immediately transferred to the cool onboard room (10-15 C°) and processed under anoxic conditions within a few hours using an argon-filled glove bag. One sediment core from each station was sectioned into 12 slices over intervals ranging from 1 to 3 cm (Fig. S2). Sediments were transferred into acid-cleaned (10 % HCl) dry polypropylene (50 ml) centrifugation tubes and spun in a refrigerated centrifuge for 20 min at 4500 rpm. The supernatant was then passed through cellulose acetate membrane syringe filters

(0.2 μm) into pre-combusted (450°C 8 hrs) clear glass ampoules for DOC and DON and amber glass vials for CDOM and FDOM. The samples were conserved and stored as described above.

Studies conducted in areas with abundant macrofauna suggested that pore waters isolated by centrifugation exhibit higher DOC concentrations compared to for non-invasive methods, such as sip-isolation (Alperin et al., 1999). Macrofauna cell rupture during centrifugation was suggested to influence the extracted DOC, and the removal of macrofauna from sediments before centrifugation and whole-core squeezing was shown to reduce elevated DOC concentrations (Martin and McCorkle, 1993). In turn, our study site did not exhibit signatures of significant bioturbation (Dale et al., 2015). Herewith, at sites similar to our study area (low oxygen - low bioturbation), DOC concentrations extracted by centrifugation were in agreement either with those obtained by sip-isolation method (Komada et al., 2004) or with those obtained from *in situ* and *ex situ* incubations (Holcombe et al., 2001). Furthermore, Holcombe et al. (2001) suggested that sip-isolated porewater DOC gradients may lead to underestimation of diffusive DOC fluxes in low-bioturbation regions. Thus, varying strength of organic matter–mineral associations may create different solute reservoirs around the surface of a mineral. Sip-isolation method was suggested to extract only loosely bound DOM out of the marine sediments, while centrifugation would sufficiently perturb sediments and sample the majority of the porewater DOM that may efflux out of the sediment. In connection with the above, the centrifugation method was preferred as pore water extraction method for DOM analyses.

2.3   Discrete sample analyses

CDOM absorbance was measured with a Shimadzu® 1700 UV-VIS double-beam spectrophotometer using a 1-cm Quartz SUPRASIL® precision cell (Hellma® Analytics). Absorbance spectra were recorded at 1 nm wavelength intervals from 230 to 750 nm against MilliQ water as a reference. CDOM absorbance spectra from 275 to 400 nm were corrected for particle scattering (e.g. Nelson and Siegel, 2013) and recalculated to absorption, according to Bricaud et al. (1981). This method has a detection limit of ∼0.001 absorption units (that may be referred to ∼0.5 m^{-1}) and a precision <5%, estimated as the maximal standard deviation of CDOM absorbance spectra from 275 to 400 nm divided by the mean value of three repeated measurements. We used the absorption coefficient at 325 nm ($a_{CDOM}(325)$) to express CDOM "concentrations", as this one is mainly used for open ocean areas (Nelson and Siegel, 2013). The spectral slope (S) for the interval 275-295 nm ($S_{275-295}$) was used to infer relative changes in DOM bulk quality, i.e. DOM relative molecular weight (Helms et al., 2008). $S_{275-295}$s were calculated following Helms et al. (2008) using log-transformed linear regression.

FDOM was analysed by Excitation-Emission Matrix (EEM) spectroscopy on a Cary Eclipse Fluorescence Spectrophotometer (Agilent Technologies) equipped with a xenon flash lamp. The fluorescence spectra for samples were measured in a 4-optical window 1-cm Quartz SUPRASIL® precision cell (Hellma®Analytics). Blank fluorescence spectra and Water Raman scans were performed daily using an Ultra-Pure Water Standard sealed cell (3/Q/10/WATER; Starna Scientific Ltd). The experimental wavelength range for sample scans and ultra-pure water scans was 230 to 455 nm in 5 nm intervals on excitation and 290 to 700 nm in 2 nm intervals on emission. Water Raman scans were recorded from 285 to 450 nm at 1 nm intervals for emission at the 275 nm excitation wavelength (Murphy et al., 2013). All fluorescence measurements were conducted at 20 °C, controlled by a Cary Single Cell Peltier Accessory (VARIAN), PMT 900 V, with 0.2 s integration times and a 5 nm slit width

on excitation and emission monochromators. The precision of this method does not exceed 3% if estimated as a standard deviation of Raman peaks at 275 nm of each measurement day, divided by the mean value. The fluorescence spectra were corrected for spectral bias, background signals and inner filter effects and normalised to the area of the ultra-pure water Raman peaks. All samples were calibrated against a Quinine Sulphate Monohydrate dilution series, performed once during sample analyses. EEMs were analysed by PARAFAC (Stedmon and Bro, 2008) and validated by split-half analysis using "drEEM toolbox for MATLAB" after Murphy et al. (2013). Four FDOM components that were identified during the PARAFAC analyses are expressed in Quinine Sulfate Equivalents (QSE).

Samples for inorganic N compounds in the benthic lander samples (NO_3^-, NO_2^- and NH_4^+) and the porewaters (NH_4^+) were analysed following standard techniques after Hansen and Koroleff (2007) and will be published elsewhere (Clemens et al., in prep.). NO_3^- and NO_2^- concentrations in the porewaters were assumed to be negligible (Dale et al., 2016) and not analysed. Detection limits for the determination of NO_3^-, NO_2^- and NH_4^+ were 0.05, 0.01, and 0.5 $\mu mol\,L^{-1}$, respectively.

DOC samples were analysed by the high-temperature catalytic oxidation (TOC -VCSH, Shimadzu) with a detection limit of 1 $\mu mol\,L^{-1}$, as described in detail by Engel and Galgani (2016). Calibration of the instrument was performed every second week using six standard solutions of 0, 500, 1000, 1500, 2500 and 5000 $\mu gC\,L^{-1}$, which were prepared using a potassium hydrogen phthalate standard (Merck 109017). Before each set of measurements, a baseline of the instrument was set using ultrapure water. The deep-sea standard (Dennis Hansell, RSMAS, University of Miami) with known DOC concentration was measured after setting the baseline to verify accuracy by the instrument. Typically, the precision of the method did not exceed 4 %. Furthermore, two control samples with known concentrations of DOC were prepared for each day of measurement using a potassium hydrogen phthalate standard (Merck 109017). The DOC concentrations of those control samples were typically within the range of samples' concentrations and were measured at the time of sample analyses to control baseline flow during measurements. The DOC concentration was determined in each sample out of five to eight replicate injections.

A TNM-1 N detector of Shimadzu analyser was used to determine TDN in parallel to DOC with a detection limit of 2 $\mu mol\,L^{-1}$ (Dickson et al., 2007). Calibration was performed simultaneously with the calibration of carbon detector using standard solutions of 0, 100, 250, 500 and 800 $\mu gN\,L^{-1}$, which was prepared using potassium nitrate Suprapur (Merck 105065). The deep-sea standard (Dennis Hansell, RSMAS, University of Miami) with the known concentration of TDN was measured daily to verify the accuracy of the instrument. The precision of the method did not exceed 2 % estimated as the standard deviation of 5–8 injections divided by the mean value. Concentrations of DON were calculated as a difference of TDN and the sum of concentrations of inorganic N components. The differences of analytical methods for determination of TDN and dissolved inorganic N species, particularly in systems dominated by dissolved inorganic N, may induce negative values during quantification of DON (Westerhoff and Mash, 2002). In this case, DON concentrations were set to "0" and, therefore, were excluded from calculations of DOC/DON ratios. In the text, those values were presented as "below detection limit (b.d.l.)".

2.4 Evaluation of DOC and DON fluxes

In this study, diffusive and *in situ* net DOC and DON fluxes were quantified. The diffusive fluxes of DOC ($J_{DOC}(Diff.)$) and DON ($J_{DON}(Diff.)$) from the uppermost slice of the sediment core (0 to 1 cm depth) to the bottom water were estimated by

applying Fick's First Law:

$$J_s(Diff.) = -\phi \times D_s \times \frac{dC}{dz} \tag{1}$$

where $J_s(Diff.)$ is a diffusive flux of a solute, ϕ is the sediment porosity, $\frac{dC}{dz}$ is the gradient of DOC (DON) concentration over the investigated depth interval (0 to 1 cm), and D_s is a bulk sediment diffusion coefficient. D_s was previously demonstrated to be dependent on the sediment formation resistivity factor (F) (Ullman and Aller, 1982), as well on the average molecular weight of DOM (Burdige et al., 1992; Balch and Guéguen, 2015). In this study, we calculate D_s using F that equals ϕ^{-3} (Ullman and Aller, 1982), as ϕ measured at 12°S exceeded 0.8-0.9 (Table 1). The molecular size fractionation was not addressed during this study, therefore, we assumed that DOM molecular weight varied in the range from 0.5 to 10 kDa. This assumption resulted in D_0 varying from 0.63×10^{-6} to 7.2×10^{-6} cm^{-2} s^{-1} (Balch and Guéguen, 2015). This variance represented one of the major drivers of the estimated diffusive DOC (DON) flux variability and was accounted for standard deviation during calculations.

Net *in situ* fluxes of DOC ($J_{DOC}(Net)$) and DON ($J_{DON}(Net)$), measured in BIGO chambers, were evaluated as:

$$J_s(Net) = \frac{V}{A} \times \frac{dC}{dt} \tag{2}$$

where $J_s(Net)$ net *in situ* flux of a solute, V is the chamber volume (in m^3), A is the chamber area (in m^2), and $\frac{dC}{dt}$ is the DOC (DON) concentration gradient over the time of the sediment enclosure (in mmol m^{-3}d^{-1}). The gradient was obtained by linear regression analyses ('polyfit' 1st order, MatLab, the MathWorks Inc.) of the DOC (DON) concentrations over time. The error of the linear regression was used as a representation of the standard deviation of the evaluated net fluxes.

In this study, fluxes directed out and into the sediment are reported as positive and negative values, respectively.

3 RESULTS

3.1 DOC and DON distribution and fluxes

Porewater DOC generally accumulated with depth in the sediment (Fig.2). Highest concentrations of DOC were measured at the middle shelf at station 1 (St.1), ranging from 152 µmol L^{-1} at 0.5 cm to a maximum of 2.6 mmol L^{-1} at 22.5 cm of sediment depth. Porewater DOC concentrations and gradients decreased gradually towards station 4 (St.4), where DOC concentrations ranged from 122 µmol L^{-1} at 0.5 cm to 544 µmol L^{-1} at 22.5 cm of sediment depth. Further offshore, porewater DOC concentrations and gradients increased at station 5 (St.5) and station 6 (St.6), ranging from 177 µmol L^{-1} at 0.5 cm to 823 µmol L^{-1} at 22.5 cm and from 210 µmol L^{-1} at 1.5 cm to 702 µmol L^{-1} at 19.5 cm, respectively. Porewater DON distribution was largely influenced by the vicinity to the coast. Highest concentrations of DON were measured at the middle shelf St.1 and St.2 (Fig.2, Fig.S7). The DON concentrations in porewaters at these stations were ranging from b.d.l. at 0.5 cm to a maximum of 2.6 mmol L^{-1} at 22.5 cm and from 580 µmol L^{-1} at 0.5 cm to 1.1 mmol L^{-1} at 19.5 cm of sediment depth, respectively. Similarly to DOC, porewater DON concentrations decreased towards St.4, where they ranged from b.d.l. at surface sediment to

85 μmol L^{-1} at 3.5 cm sediment depth and then resumed the gradient offshore at St.5 (64–450 μmol L^{-1}) and St.6 (b.d.l.–248 μmol L^{-1}).

Sediment porewaters at 12°S exhibited low DOC/DON ratios. The median DOC/DON ratio for most of the stations fell below 5. Generally, the median elemental ratio increased towards offshore from the minimum at St.2 (DOC/DON of <1) to maximum at St.4 (median DOC/DON ~12) and then decreased again at St.5 (median DOC/DON ~1) and St.6 (median DOC/DON ~3) (Fig.S3).

Near-bottom waters in the benthic incubation chambers did not display apparent differences in DOC concentrations between stations (Fig. 3). Average concentrations were 92±22 μmol L^{-1}. Furthermore, DOC did not accumulate linearly over time at some stations (Fig.3). Similarly, DON concentrations varied from b.d.l. to ~15 μmol L^{-1} in the chambers (Fig.3), resulting in much higher DOC/DON ratios than measured in the porewaters. Median DOC/DON ratios in all chambers were >5, gradually decreasing from a maximum at St.1 (median DOC/DON ~30) towards offshore (Fig.S3).

The diffusive DOC fluxes varied from a minimum of 0.2±0.1 mmol m^{-2}d^{-1} at St.2 to a maximum of 2.5±1.3 mmol m^{-2}d^{-1} at station 3 (St.3) (Fig. 4). Net *in situ* DOC fluxes determined with benthic chambers were generally lower than diffusive fluxes and varied from -0.3±0.9 at St.4 to 2.3±2.3 mmol m^{-2}d^{-1} at St.2. However, no statistical differences were found between the different flux estimates at each station (*p*>0.05, Mann-Whitney Rank Sum Test, SigmaPlot, Systat Software). Diffusive DON fluxes ranged from -0.04±0.02 mmol m^{-2}d^{-1} at St.1 and St.6 to 3.3±1.7 mmol m^{-2}d^{-1} at St.2. Similar to DOC, net *in situ* DON fluxes were lower than diffusive DON fluxes and ranged from -0.05±0.3 mmol m^{-2}d^{-1} at St.6 to 0.3±0.3 mmol m^{-2}d^{-1} at St.5.

3.2   Optical properties of DOM

To address DOM quality CDOM and FDOM fluorescence intensities were analysed in the sediment porewaters and in the BIGO chambers.

In the porewaters, CDOM absorption (a$_{CDOM}$(325)) exhibited a similar pattern to DOC distribution (Fig.2). Highest a$_{CDOM}$(325)s were measured at St.1. They ranged from 3.2 m^{-1} at 0.5 cm to 22.8 m^{-1} at 22.5 cm of sediment depth. The lowest a$_{CDOM}$(325)s were measured at St.4, ranging from 2.7 m^{-1} at 0.5 cm to 8.9 m^{-1} at 7 cm of sediment depth. Further offshore, at St.5 and St.6 a$_{CDOM}$(325)s were higher than at St.4, resuming the offshore gradient.

In the benthic chambers, at the outer shelf and continental slope, a$_{CDOM}$(325)s generally ranged from 0.3 to 2.5 m^{-1} (Fig.3), exhibiting, however, different trends. Thus, an apparent decrease of a$_{CDOM}$(325) over time occurred at St.3, St.5 and St.6, while at St.4 a$_{CDOM}$(325) exhibited an apparent accumulation. Middle shelf stations, St.1 and St.2, displayed lower variance, ranging from 0.1 to 1 over time, and exhibited no visible trends (Fig.3, Table S1).

CDOM spectral slope, S$_{275-295}$, in the porewaters increased with depth in all sediment cores, displaying highest values (-0.016±0.004 nm^{-1}) at St.4, and the lowest values at St.1 S$_{275-295}$ (-0.018±0.001 nm^{-1}). The latter were comparable to the initial values of S$_{275-295}$ in the BIGO benthic chambers (-0.018±0.005 nm^{-1}) (see Fig.2 and Fig.3).

In all the BIGO chambers, highest S$_{275-295}$ were observed at the beginning of sediment enclosure, and an apparent S$_{275-295}$ decrease occurred over time (Fig. 3). The decrease in S$_{275-295}$ was steeper at stations with higher porewater DOC content.

Thus, the fastest change in $S_{275\text{-}295}$ occurred at St.1 (-0.016±0.017 $\text{nm}^{-1}\text{d}^{-1}$) whereas slowest change was found at St.4 (-0.004±0.006 $\text{nm}^{-1}\text{d}^{-1}$). (Fig.3, Table S1).

FDOM spectroscopy and PARAFAC analyses allowed four independent fluorescent components to be distinguished (Fig.5). FDOM components that are excited at UV and emit in the visible spectra were previously referred to as humic-like substances
(e.g., Coble, 1996; Murphy et al., 2013, 2014; Loginova et al., 2016, and references therein). Here, two fluorescent components, FDOM component 1 (Comp.1) and FDOM component 2 (Comp.2), with excitation and emission (Ex/Em) of 370/464 nm and 290-325/400 nm, respectively, were referred to as humic-like components (Fig. 5). Amino acid-like substances are the second group of well-determined FDOM components (e.g., Coble, 1996; Murphy et al., 2013, 2014; Loginova et al., 2016, and references therein) corresponding to molecules that are excited and emit in the UV spectra. Thus, FDOM component 3
(Comp.3) and FDOM component 4 (Comp.4), with Ex/Em of 290/340(684) nm and 275/310(600) nm, respectively, were assumed to represent proteinaceous DOM (Fig. 5). During this study, humic-like components showed similar trends to DOC and $a_{\text{CDOM}}(325)$ in the porewaters. Their fluorescence accumulated with sediment core depth and decreased offshore with a minimum fluorescence at St.4 (Fig.6). Amino acid-like Comp.3 and Comp.4, also accumulated in the porewaters, but were generally depleted throughout the sediment except for St.1, where their fluorescence reached max. 6 QSE and max. 1.7 QSE,
respectively (Fig.6).

In the benthic chambers, all fluorescent component QSEs were nearly an order of magnitude lower than those in the pore-waters. An apparent accumulation within chambers was observed for humic-like Comp.1 and Comp.2 and amino acid-like Comp.4 (Fig.7). Comp.3 displayed a slight apparent accumulation at the beginning of the sediment incubation followed by an apparent removal at a later stage on St.1, St.3, St.4 and St.6. Humic-like Comp.1, Comp.2 and amino acid-like Comp.4 dis-
played similar gradients among nearly all the stations of ~0.03, 0.06–0.08 and 0.03–0.04 $\text{QSE}\,\text{d}^{-1}$, respectively. Exceptions were St.4 which displayed Comp.1,Comp.2 and Comp.4 gradients of 0.001, 0.04 and -0.005 $\text{QSE}\,\text{d}^{-1}$, respectively; and St.1, where the gradients of Comp.2 and Comp.4 were ~0.04 and ~0.09 $\text{QSE}\,\text{d}^{-1}$, respectively (Table S1).

4   DISCUSSION

4.1   Spatial variability of the DOM fluxes at 12ºS transect

Spatial variability of organic matter decomposition in sediments is a common feature in the world ocean (see Arndt et al., 2013, for an overview). This variability is naturally attributed to the efficiency of vertical transfer of POM to the sediment (e.g. Seiter et al., 2004; Marsay et al., 2015; Engel et al., 2017). At 12ºS, highest sedimentation rates, estimated via $^{210}Pb_{xs}$ activity were reported for the middle shelf St.1 and St.2, while St.4 displayed the lowest sedimentation rates and porewater DOM concentrations possibly caused by an inhibition of particle settling by bottom currents (Dale et al., 2015). The highest accu-
mulation of POM at 12ºS was also observed at St.1 and St.2 even though the organic carbon burial efficiency exhibited lower values at the middle shelf stations than the stations offshore (Dale et al., 2015). Lower carbon burial efficiency in combination with very high rates of organic matter remineralisation, as follows from extremely high DIC and NH_4^+ benthic fluxes (Dale et al., 2015; Sommer et al., 2016), suggests higher bioavailability of POM supplied to the middle shelf. Accordingly, porewater

DOM optical properties reflected the "freshest" character of organic matter at St.1 and St.2, where $S_{275-295}$ displayed similar properties to those in the water column (Fig. 3) and protein-like DOM fluorescence (Fig. 6) and DON were highly enriched (Fig. 3). Therefore, in line to the previous findings, our data suggests that the middle shelf stations are supplied with more labile POM compared to the outer shelf stations. This labile POM, likely of proteinaceous origin (e.g. Faganeli and Herndl,

5   1991), is rapidly reworked, resulting in greater DOM release at the middle shelf stations. Despite the highest sediment accumulation and POC mineralisation rates at St.1 (Dale et al., 2015) and elevated porewater DOC and especially DON concentrations (Fig. 8, Fig.S7), the diffusive fluxes of DOC and DON here were not highest on the transect. As $a_{CDOM}(325)$ and protein-like FDOM was previously related to the dynamics of labile DOM (Loginova et al., 2016), one may expect those fractions to be rapidly reworked by heterotrophic communities. Therefore, little dynamics of optical properties of proteinaceous character

10   and $a_{CDOM}(325)$ might be a result as of the absence of benthic labile DOM fluxes, but also a signature of rapid microbial utilisation of labile organic matter freshly released from the sediment (Komada et al., 2016). Thus, the greatest decrease in $S_{275-295}$ and accumulation of humic-like substances also suggest that benthic release of fresh bioavailable DOM at St.1 should be rapidly and extensively reworked or consumed at the sediment-water column interface during the time of incubations. These results support the idea that microbial utilisation is controlled by the quality of supplied organic matter (Pantoja et al., 2009;

15   Le Moigne et al., 2017). On the other hand, the spatial flux variability could also be attributed to the spatially variable DOM recycling efficiencies of different biogeochemical processes. For instance, denitrification and anammox were found to be the major processes of N cycling in the outer shelf and on the upper continental slope, whereas middle shelf stations, had elevated rates of DNRA (Dale et al., 2016; Sommer et al., 2016). While the linkages between microbial N turnover and DOM fluxes are unclear, it is noteworthy that the middle shelf sediments were covered with *Marithioploca* mats that greatly affect the N and

20   sulphur biogeochemical cycles and, potentially, DOM cycling and reactivity.

At St.2, DON accumulated to higher levels than DOC and NH_4^+ within the porewaters (see e.g. Fig. S7), leading to higher diffusive DON fluxes than those of DOC and extremely low DOC/DON ratios (Fig. S3). In agreement to this $S_{275-295}$ revealed lowest changes over time, suggesting that DOM at benthic chamber at St.2 remained "fresher" during the time of incubations, compared to other stations. Similar to that, proteinaceous Comp.3, despite its generally low variability, exhibited highest

25   increase at St.2, suggesting relative accumulation of proteinaceous DOM in the corresponding chamber. Herewith, porewater DON concentrations generally seemed to be more influenced by the vicinity to the fresh organic matter source, while porewater DOC accumulated proportionally to the organic matter degradation along with the increase of sediment depth, as indicated by NH_4^+ concentrations (Fig.S7). Those results are in line with previously suggested "decoupling" between DOC and DON remineralisation mechanisms by e.g. Alkhatib et al. (2013), that was ascribed to POM reactivity. Thus, the authors suggested

30   that the enzymatic hydrolysis of N-containing labile POM occurs at a higher rate than that of carbon-rich compounds, leading to lower an accumulation of DON over DOC in the porewaters. Furthermore, the dissolved by-products of bacterial activity are often found to be enriched in N, and therefore the sediments where microbial activity is pronounced show relatively low values of DOC/DON ratios (Burdige and Komada, 2015). Thus, glycine (DOC/DON=2) was suggested to preferentially accumulate as a result of microbial metabolism in mixed redox sediments (Burdige, 2002). Bioturbation by macro-biota in oxygenated

35   sediments is also often associated with the accumulation of urea (DOC/DON=0.5) (Burdige and Gardner, 1998). However,

given that retrieved sediment cores were apparently not bioturbated, active remineralisation of bioavailable organic matter by microbial communities within the sediment is more likely. In addition, DOM itself may enter chemical reactions with hydrogen sulphide that is produced in large quantities at middle shelf stations (Schunck et al., 2013; Sommer et al., 2016). For instance, quinone structures can react with hydrogen sulphide, producing hydroquinones (Heitmann and Blodau, 2006), which may be

5 further utilised by methanogenic degradation processes (Szewzyk et al., 1985). This could affect DOC and DON porewater concentrations and decrease the diffusive DOC flux over the diffusive DON flux. However, the extreme accumulation of DON over the DOC in porewaters at St.2 and also St.1 seem to be hardly explainable with the organic N sources alone. Herewith, our arguments are likely speculative, and the actual mechanism behind decoupling of DOC and DON fluxes remains obscure.

4.2 Porewater DOM and its near-bottom utilisation at the near coastal waters off Peru

10 In classical understanding, production of DOM from POM degradation processes followed by slow microbial utilisation of DOM (e.g. Burdige and Komada, 2015) causes an imbalance in DOM production and consumption, resulting in a net accumulation of DOM with sediment depth. This is commonly explained by an accumulation of recalcitrant LMWDOM in the sediments produced by "microbial pump" (Burdige and Komada, 2015). Furthermore, physico-chemical processes, such as: 1) irreversible sorption onto particles, 2) aggregation (Liu and Lee, 2007; Arndt et al., 2013), 3) reactions of chelation and

15 4) co-precipitation (Lalonde et al., 2012), or 5) an inhibition of microbial activity (Emerson, 2013; Canfield, 1994; Aller and Aller, 1998) may contribute to the DOM accumulation in sediment porewaters. On the other hand, isotopic carbon composition of the porewater DOM suggests that its substantial fraction is isotopically young and is readily utilised by heterotrophic communities, when released to the water column (Bauer et al., 1995; Komada et al., 2013; Burdige et al., 2016). The observed accumulation of DOM with depth in porewaters in this study (Fig. 2) agrees well with previous observations (Burdige and

20 Gardner, 1998; Komada et al., 2004; Chipman et al., 2010; Alkhatib et al., 2013) as well as with reported DOC concentrations in non-bioturbated anoxic sediments ($\sim$1-3 $\mathrm{mmol\,l^{-1}}$) (Burdige and Komada, 2015). The accumulation of humic-like fluorescence and its correlation with DOC concentrations (Comp.1, R=0.8, n=0.86, p<0.01), as observed during our study, has also been noted previously in marine sediments (e.g. Chen et al., 1993). The increase of the humic-like fluorescence with sediment depth is commonly explained as a net production of LMW recalcitrant humic DOM and an increasing fraction of FDOM in

25 the porewaters compared to the water column (Komada et al., 2004). The increase of $S_{275\text{-}295}$ over sediment depth indicated an increase of apparent molecular weight (Helms et al., 2008). This apparent increase of molecular weight in combination with the down-core enrichment in humic-like fluorescence suggests an accumulation of so-called polymeric LMW (pLMW) DOM. This may be formed via reactions of polymerisation (Hedges et al., 1988) or complexation (Finke et al., 2007), as well as due to formation of supramolecular clusters via hydrogen bonding or hydrophobic interactions (e.g. Sutton and Sposito,

30 2005). The down-core accumulation of DON and amino acid-like FDOM, and also correlation of amino acid-like FDOM to DOC (Comp.4, R=0.6, n=0.86, p<0.01) suggest that proteinaceous DOM is also being produced during POM remineralisation in sediments. Given that the second emission peaks of Comp.3 and Comp.4 displayed similar spectral characteristics to chl *a* and its auxiliary carotenoids (e.g. Wolf and Stevens, 1967), the protein-like FDOM components are likely products of phytoplankton debris recycling.

Benthic DOM fluxes were previously shown to constitute an important fraction of the organic matter that escapes remineralisation in the sediments (e.g. Ludwig et al., 1996; Burdige et al., 1999). Net *in situ* benthic DOC fluxes found during our study (-0.3 ± 0.9–2.3 ± 2.3 mmol m^{-2}d^{-1}) (Fig. 8) were comparable to previous estimates for shelf and continental slope sediments off coast of Peru and California, ranging from 0.03–4.41 mmol m^{-2}d^{-1} (see Burdige et al., 1992, 1999; Burdige and Komada, 2015, for full overview). However, the common assumption of linear accumulation of DOC and DON in benthic chambers (Burdige et al., 1992; Burdige and Homstead, 1994; Burdige et al., 1999) over time was generally not met. We were able to trace the qualitative transformations of DOM in benthic chambers over the investigated time period by the changes in DOM optical properties. The decrease of S$_{275\text{-}295}$ along with the enrichment in humic-like fluorescence over time indicated an accumulation of LMW humic DOM components (Helms et al., 2008), while the complex development of the amino acid-like fluorescence of Comp.3 and the drawdown of a$_{CDOM}$(325) and also of DON, resulting in increased DOC/DON ratios, suggested reworking of proteinaceous labile DOM in benthic chambers during the investigated time period (Fig.8). Thus, the production of humic-like LMWDOM along with the utilisation of proteinaceous DOM suggest active microbial DOM utilisation occurring in the near-bottom waters. Therefore our results from the benthic chambers support the idea that DOM release to the water column may stimulate respiration by water column microbial communities (Alkhatib et al., 2013; Komada et al., 2016; Burdige et al., 2016).

As stated previously, the rate of organic matter decomposition in sediments may be dependent not only on organic matter bioavailability (Canfield, 1994), but also on inhibition of microbial activity (Aller and Aller, 1998), and availability of electron acceptors (Emerson, 2013; Canfield, 1994). We suggest that the availability of electron acceptors, such as NO$_3^-$ and NO$_2^-$, in the water column above the sediments (Thomsen et al., 2016; Lüdke et al., 2019, and also Fig. S6) could stimulate near-bottom microbial communities to take up DOM, for instance, as a result of predominant on the outer shelf and continental slope denitrification as follows from the rapid NO$_3^-$ and NO$_2^-$ uptake by the sediments (Fig. S6; Dale et al., 2016). Furthermore, the formation of pLMWDOM due to geo-polymerisation, the formation of supra-molecules due to hydrogen bonding (Sutton and Sposito, 2005; Finke et al., 2007) or encapsulation by humic substances (e.g. Tomaszewski et al., 2011) may reduce accessibility of bioavailable DOM compounds in sediments. Labile substances, such as amino acids and carbohydrates, may become unavailable for heterotrophic communities within the porewaters, resulting in DON accumulation with sediment depth. Herewith, the subsequent release of pLMWDOM into the water column may lead to unfolding (solubilisation) of those supra-molecules due to, e.g. the chaotropic effect of NO$_3^-$ (e.g. Gibb and Gibb, 2011), and, consequently, increase DOM bioavailability for the near-bottom microbial communities.

Therefore, a non-conservative behaviour of DOC and DON and proteinaceous FDOM in the BIGO chambers during sediment enclosure might be a result of sediment release/microbial DOM consumption and reworking in the near-bottom waters or the sediment-water column interface. Furthermore, DOM released by the sediment could potentially support an enhanced microbial abundance and carbon oxidation rates reported near the sediment on 12°S transect (Maßmig et al., 2020) and influence the activity of microbial mats that cover up to 100 % of the sediment surface at the middle shelf stations (Sommer et al., 2016). In turn, POM respiration rates, which are commonly evaluated from DIC flux measured in benthic lander systems (Dale et al., 2015), may have an input as from sediment release of DIC as from the *in situ* DIC production via DOM remineralisation. Given

that the diffusive DOC fluxes, calculated in this study could represent up to $\sim$53 % of the estimated DIC flux (J_{DIC}, Clements et al., in prep.), while the net *in situ* benthic DOC fluxes could describe only up to $\sim$28 % of J_{DIC}, POM remineralisation rates estimated from net *in situ* DIC flux will be subjected to less bias, caused by the ignorance of DOM sediment release by previous studies. On the other hand, however, whether all the DOM utilisation that takes place within benthic chambers in our study is actually bound to the sediment-water interface is not completely clear. Thus, the enclosure of sediment over a period of $\sim$30 hrs may block out near bottom currents (e.g. Lüdke et al., 2019) and other mechanisms of lateral transport, e.g. eddies (Thomsen et al., 2016), that might influence the water column distribution of the freshly released from sediments DOM. For instance, Lüdke et al. (2019) reported near bottom poleward flow ranging from 0.1 to 0.4 $\mathrm{m\,s^{-1}}$. That could imply, that, at stable flow, DOM, which have been released by the sediment, could be distributed along with a distance of 10 to 40 km during the time equivalent to the time of sediment enclosure by BIGO chambers. Furthermore, Loginova et al. (2016) reported an apparent transport of similar by spectral properties to Comp.1 humic-like fluorescence to the surface waters at the beginning of their cruise. Therefore, DOM released to the bottom waters may be not limited only to the sediment-water column interface, affecting whole water column biogeochemistry.

We suggest that the difference between the diffusive flux and net *in situ* flux could reflect the rate of microbial DOC utilisation in the chamber water and/or surface sediment layer at each station. Thus, we estimated rates of microbial utilisation at St.3-St.6 ranging from 0.2 to 1.7 $\mathrm{mmol\,m^{-2}d^{-1}}$ (Fig.8). We here propose to link these utilisation rates to rates of denitrification. Evidences from fieldwork suggest that at least part of the denitrification occurring at depth may be driven by the supply of POM via the biological carbon pump (Liu and Kaplan, 1984; Kalvelage et al., 2013). Other suggested that DOM supply could also stimulate denitrification in oxygen deficient zones (e.g. Chang et al., 2014; Bonaglia et al., 2016). Given the importance of denitrification and N-loss rates for OMZ regions, it is crucial to evaluate various possible sources of organic matter potentially sustaining such rates. By conversion of the remineralisation rates of outfluxed DOM, found in our study (Fig.8), into denitrification rates using stoichiometry previously reported by Prokopenko et al. (2011), we estimated associated denitrification rates ranging from 0.2 to 1.4 $\mathrm{mmol\,m^{-2}d^{-1}}$. These are comparable to denitrification rates ($\sim$0.6 $\mathrm{mmol\,m^{-2}d^{-1}}$) and the total $\mathrm{N_2}$ efflux ($\sim$1.2 $\mathrm{mmol\,m^{-2}d^{-1}}$) reported in anoxic sediments in the eastern tropical North Pacific off California (Prokopenko et al., 2011), to denitrification rates (0.2–2 $\mathrm{mmol\,m^{-2}d^{-1}}$) in the eastern tropical North Atlantic off Mauritania (Dale et al., 2014) and to modelled denitrification rates (0.5–1.1 $\mathrm{mmol\,m^{-2}d^{-1}}$) and $\mathrm{N_2}$ fluxes (0.8–4.6 $\mathrm{mmol\,m^{-2}d^{-1}}$), observed along 12ºS transect (Dale et al., 2015; Sommer et al., 2016). Our estimates could, in turn, explain between 5 and 45 % of denitrification rates measured in the water column in the eastern tropical South Pacific ($\sim$3 $\mathrm{mmol\,m^{-2}d^{-1}}$; (Kalvelage et al., 2013)). Therefore we suggest that sediment release of DOC is not the dominant source of organic matter to the OMZ, but on occasions, this process may potentially serve as an important source of organic matter for the water column N–loss.

5   Conclusions

Diffusive fluxes of DOC and DON displayed high spatial variability, which was likely caused by the quality of DOM supplied to the sediment and by differences in mechanisms of microbial metabolism at different water depths, suggested in the previous

studies. A general decrease of net *in situ* DOC and DON fluxes, compared to diffusive fluxes as well as an apparent steepening of $S_{275\text{-}295}$ and accumulation of humic-like material within benthic chambers during the time of the sediment enclosure at all stations suggest that released to the water column DOM is being actively reworked near the sediment. The near-bottom remineralisation of DOM is, likely, stimulated by high availability of strong electron acceptors, such as NO_3^- and NO_2^-, in the water column at the outer shelf and continental slope stations. The utilisation of DOC released by the sediment, in turn, may account for denitrification rates, comparable to previously reported for the water column and sediments off Peru and other OMZs, suggesting sediment release to be a potentially important source of bioavailable DOM for the near-bottom microbial communities.

Data availability. All the measured DOC concentrations, $a_{CDOM}(325)$, $S_{275\text{-}295}$ and QSE of fluorescent components will be available at pangaea.de with the link to the project: SFB754 upon publication

Author contributions. ANL designed the sampling strategy and analysed DOM samples. AWD collected samples at MUC and BIGO stations and provided data for calculation of fluxes, ST helped with water sampling, DC provided inorganic N data, SS helped with the sampling strategy design and sampling and also provided all the facilities for sampling from BIGO landers, KW provided the initial idea for the research. ANL wrote the manuscript with contributions from AWD, FACLM, ST, SS, and AE.

Competing interests. The authors are not aware of competing interests of any sort for this research.

Acknowledgements. We are grateful to the chief scientists M. Dengler and ship and scientific crews of RV Meteor (cruises M136 and M137). J. Roa is acknowledged for DOC analyses. We are grateful to B. Domeyer, A. Bleyer, M. Türk and A. Beck for technical and logistical support, and to D. Clements and U. Schroller-Lomnitz for advice and data support.

This research has been supported by the Deutsche Forschungsgemeinschaft (DFG) grant no.: SFB754 "Climate-Biogeochemical Interactions in the Tropical Ocean" (miniproposal, B9) and funding provided by Inge-Lehmann-Fonds through GEOMAR Helmholtz Centre for Ocean Research awarded to ANL and by DFG Excellence cluster Future Ocean CP1403 "Transfer and remineralisation of biogenic elements in the tropical oxygen minimum zones" awarded to FACLM. ST was supported by the European Commission (Horizon 2020, MSCA-IF-2016, WACO 749699: Fine-scale Physics, Biogeochemistry and Climate Change in the West AfricanCoastal Ocean).

References

Alkhatib, M., del Giorgio, P. A., Gelinas, Y., and Lehmann, M. F.: Benthic fluxes of dissolved organic nitrogen in the lower St. Lawrence estuary and implications for selective organic matter degradation, Biogeosciences, 10, 7609–7622, https://doi.org/10.5194/bg-10-7609-2013, https://www.biogeosciences.net/10/7609/2013/, 2013.

5 Aller, R. C. and Aller, J. Y.: The effect of biogenic irrigation intensity and solute exchange on diagenetic reaction rates in marine sediments, Journal of Marine Research, 56, 905–936, https://doi.org/10.1357/002224098321667413, https://www.ingentaconnect.com/content/jmr/jmr/1998/00000056/00000004/art00008, 1998.

Alperin, M. J., Martens, C. S., Albert, D. B., Suayah, I. B., Benninger, L. K., Blair, N. E., and Jahnke, R. A.: Benthic fluxes and porewater concentration profiles of dissolved organic carbon in sediments from the North Carolina continental slope, Geochimica et Cosmochim-

10 ica Acta, 63, 427 – 448, https://doi.org/https://doi.org/10.1016/S0016-7037(99)00032-0, http://www.sciencedirect.com/science/article/pii/S0016703799000320, 1999.

Arévalo-Martínez, D. L., Kock, A., Löscher, C. R., Schmitz, R. A., and Bange, H. W.: Massive nitrous oxide emissions from the tropical South Pacific Ocean, Nature Geoscience, 8, 530 EP –, https://doi.org/10.1038/ngeo2469, 2015.

Arndt, S., Jørgensen, B., LaRowe, D., Middelburg, J., Pancost, R., and Regnier, P.: Quantifying the degradation of organic matter in marine

15 sediments: A review and synthesis, Earth-Science Reviews, 123, 53 – 86, https://doi.org/10.1016/j.earscirev.2013.02.008, http://www.sciencedirect.com/science/article/pii/S0012825213000512, 2013.

Balch, J. and Guéguen, C.: Effects of molecular weight on the diffusion coefficient of aquatic dissolved organic matter and humic substances, Chemosphere, 119, 498 – 503, https://doi.org/10.1016/j.chemosphere.2014.07.013, http://www.sciencedirect.com/science/article/pii/S0045653514008637, 2015.

20 Bauer, J. E., Reimers, C. E., Druffel, E. R. M., and Williams, P. M.: Isotopic constraints on carbon exchange between deep ocean sediments and sea water, Nature, 373, 686–689, https://doi.org/10.1038/373686a0, https://doi.org/10.1038/373686a0, 1995.

Belzile, C., Gibson, J. A. E., and Vincent, W. F.: Colored dissolved organic matter and dissolved organic carbon exclusion from lake ice: Implications for irradiance transmission and carbon cycling, Limnology and Oceanography, 47, 1283–1293, https://doi.org/10.4319/lo.2002.47.5.1283, https://aslopubs.onlinelibrary.wiley.com/doi/abs/10.4319/lo.2002.47.5.1283, 2002.

25 Bohlen, L., Dale, A., Sommer, S., Mosch, T., Hensen, C., Noffke, A., Scholz, F., and Wallmann, K.: Benthic nitrogen cycling traversing the Peruvian oxygen minimum zone, Geochimica et Cosmochimica Acta, 75, 6094 – 6111, https://doi.org/https://doi.org/10.1016/j.gca.2011.08.010, http://www.sciencedirect.com/science/article/pii/S0016703711004662, 2011.

Bonaglia, S., Klawonn, I., De Brabandere, L., Deutsch, B., Thamdrup, B., and Brüchert, V.: Denitrification and DNRA at the Baltic Sea oxic–anoxic interface: Substrate spectrum and kinetics, Limnology and Oceanography, 61, 1900–1915, https://doi.org/10.1002/lno.10343,

30 https://aslopubs.onlinelibrary.wiley.com/doi/abs/10.1002/lno.10343, 2016.

Bricaud, A., Morel, A., and Prieur, L.: Absorption by dissolved organic matter of the sea (yellow substance) in the UV and visible domains1, Limnology and Oceanography, 26, 43–53, https://doi.org/10.4319/lo.1981.26.1.0043, https://aslopubs.onlinelibrary.wiley.com/doi/abs/10.4319/lo.1981.26.1.0043, 1981.

Burdige, D. J.: Chapter 13 - Sediment Pore Waters, in: Biogeochemistry of Marine Dissolved Organic Matter, edited by Hansell, D. A.

35 and Carlson, C. A., pp. 611 – 663, Academic Press, San Diego, https://doi.org/https://doi.org/10.1016/B978-012323841-2/50015-4, http://www.sciencedirect.com/science/article/pii/B9780123238412500154, 2002.

Burdige, D. J. and Gardner, K. G.: Molecular weight distribution of dissolved organic carbon in marine sediment pore waters, Marine Chemistry, 62, 45 – 64, https://doi.org/10.1016/S0304-4203(98)00035-8, http://www.sciencedirect.com/science/article/pii/S0304420398000358, 1998.

Burdige, D. J. and Homstead, J.: Fluxes of dissolved organic carbon from Chesapeake Bay sediments, Geochimica et Cosmochimica Acta, 58, 3407 – 3424, https://doi.org/10.1016/0016-7037(94)90095-7, http://www.sciencedirect.com/science/article/pii/0016703794900957, 1994.

Burdige, D. J. and Komada, T.: Chapter 12 - Sediment Pore Waters, in: Biogeochemistry of Marine Dissolved Organic Matter (Second Edition), edited by Hansell, D. A. and Carlson, C. A., pp. 535 – 577, Academic Press, Boston, second edition edn., https://doi.org/10.1016/B978-0-12-405940-5.00012-1, http://www.sciencedirect.com/science/article/pii/B9780124059405000121, 2015.

Burdige, D. J., Alperin, M. J., Homstead, J., and Martens, C. S.: The Role of Benthic Fluxes of Dissolved Organic Carbon in Oceanic and Sedimentary Carbon Cycling, Geophysical Research Letters, 19, 1851–1854, https://doi.org/10.1029/92GL02159, https://agupubs.onlinelibrary.wiley.com/doi/abs/10.1029/92GL02159, 1992.

Burdige, D. J., Berelson, W. M., Coale, K. H., McManus, J., and Johnson, K. S.: Fluxes of dissolved organic carbon from California continental margin sediments, Geochimica et Cosmochimica Acta, 63, 1507 – 1515, https://doi.org/10.1016/S0016-7037(99)00066-6, http://www.sciencedirect.com/science/article/pii/S0016703799000666, 1999.

Burdige, D. J., Komada, T., Magen, C., and Chanton, J. P.: Modeling studies of dissolved organic matter cycling in Santa Barbara Basin (CA, USA) sediments, Geochimica et Cosmochimica Acta, 195, 100 – 119, https://doi.org/https://doi.org/10.1016/j.gca.2016.09.007, http://www.sciencedirect.com/science/article/pii/S001670371630521X, 2016.

Canfield, D. E.: Factors influencing organic carbon preservation in marine sediments, Chemical Geology, 114, 315 – 329, https://doi.org/10.1016/0009-2541(94)90061-2, http://www.sciencedirect.com/science/article/pii/0009254194900612, 1994.

Catalá, T. S., Álvarez Salgado, X. A., Otero, J., Iuculano, F., Companys, B., Horstkotte, B., Romera-Castillo, C., Nieto-Cid, M., Latasa, M., Morán, X. A. G., Gasol, J. M., Marrasé, C., Stedmon, C. A., and Reche, I.: Drivers of fluorescent dissolved organic matter in the global epipelagic ocean, Limnology and Oceanography, 61, 1101–1119, https://doi.org/10.1002/lno.10281, https://aslopubs.onlinelibrary.wiley.com/doi/abs/10.1002/lno.10281, 2016.

Chang, B. X., Rich, J. R., Jayakumar, A., Naik, H., Pratihary, A. K., Keil, R. G., Ward, B. B., and Devol, A. H.: The effect of organic carbon on fixed nitrogen loss in the eastern tropical South Pacific and Arabian Sea oxygen deficient zones, Limnology and Oceanography, 59, 1267–1274, https://doi.org/10.4319/lo.2014.59.4.1267, https://aslopubs.onlinelibrary.wiley.com/doi/abs/10.4319/lo.2014.59.4.1267, 2014.

Chen, M., Kim, J.-H., Nam, S.-I., Niessen, F., Hong, W.-L., Kang, M.-H., and Hur, J.: Production of fluorescent dissolved organic matter in Arctic Ocean sediments, Scientific Reports, 6, 39 213 EP –, https://doi.org/10.1038/srep39213, article, 2016.

Chen, R. F., Bada, J. L., and Suzuki, Y.: The relationship between dissolved organic carbon (DOC) and fluorescence in anoxic marine porewaters: Implications for estimating benthic DOC fluxes, Geochimica et Cosmochimica Acta, 57, 2149 – 2153, https://doi.org/10.1016/0016-7037(93)90102-3, http://www.sciencedirect.com/science/article/pii/0016703793901023, 1993.

Chipman, L., Podgorski, D., Green, S., Kostka, J., Cooper, W., and Huettel, M.: Decomposition of plankton-derived dissolved organic matter in permeable coastal sediments, Limnology and Oceanography, 55, 857–871, https://doi.org/10.4319/lo.2010.55.2.0857, https://aslopubs.onlinelibrary.wiley.com/doi/abs/10.4319/lo.2010.55.2.0857, 2010.

Coble, P. G.: Characterization of marine and terrestrial DOM in seawater using excitation-emission matrix spectroscopy, Marine Chemistry, 51, 325 – 346, https://doi.org/10.1016/0304-4203(95)00062-3, http://www.sciencedirect.com/science/article/pii/0304420395000623, 1996.

Dale, A., Sommer, S., Ryabenko, E., Noffke, A., Bohlen, L., Wallmann, K., Stolpovsky, K., Greinert, J., and Pfannkuche, O.: Benthic nitrogen fluxes and fractionation of nitrate in the Mauritanian oxygen minimum zone (Eastern Tropical North Atlantic), Geochimica et Cosmochimica Acta, 134, 234 – 256, https://doi.org/10.1016/j.gca.2014.02.026, http://www.sciencedirect.com/science/article/pii/S0016703714001331, 2014.

5 Dale, A., Sommer, S., Lomnitz, U., Bourbonnais, A., and Wallmann, K.: Biological nitrate transport in sediments on the Peruvian margin mitigates benthic sulfide emissions and drives pelagic N loss during stagnation events, Deep Sea Research Part I: Oceanographic Research Papers, 112, 123 – 136, https://doi.org/10.1016/j.dsr.2016.02.013, http://www.sciencedirect.com/science/article/pii/S0967063715301308, 2016.

Dale, A. W., Sommer, S., Lomnitz, U., Montes, I., Treude, T., Liebetrau, V., Gier, J., Hensen, C., Dengler, M., Stolpovsky, K., Bryant, L. D.,
10 and Wallmann, K.: Organic carbon production, mineralisation and preservation on the Peruvian margin, Biogeosciences, 12, 1537–1559, https://doi.org/10.5194/bg-12-1537-2015, https://www.biogeosciences.net/12/1537/2015/, 2015.

Del Vecchio, R. and Blough, N. V.: On the Origin of the Optical Properties of Humic Substances, Environmental Science & Technology, 38, 3885–3891, https://doi.org/10.1021/es049912h, https://doi.org/10.1021/es049912h, 2004.

Demaison, G. and Moore, G.: Anoxic environments and oil source bed genesis, Organic Geochemistry, 2, 9 – 31,
15 https://doi.org/10.1016/0146-6380(80)90017-0, http://www.sciencedirect.com/science/article/pii/0146638080900170, 1980.

Dickson, A. G., Sabine, C. L., and Christian, J. R.: Guide to best practices for ocean CO2 measurements, 2007.

Emerson, S.: Organic Carbon Preservation in Marine Sediments, pp. 78–87, American Geophysical Union (AGU), https://doi.org/10.1029/GM032p0078, https://agupubs.onlinelibrary.wiley.com/doi/abs/10.1029/GM032p0078, 2013.

Engel, A. and Galgani, L.: The organic sea-surface microlayer in the upwelling region off
20 the coast of Peru and potential implications for air–sea
exchange processes, Biogeosciences, 13, 989–1007, https://doi.org/10.5194/bg-13-989-2016, https://www.biogeosciences.net/13/989/2016/, 2016.

Engel, A., Wagner, H., Le Moigne, F. A. C., and Wilson, S. T.: Particle export fluxes to the oxygen minimum zone
of the eastern tropical North Atlantic, Biogeosciences, 14, 1825–1838, https://doi.org/10.5194/bg-14-1825-2017, https://www.
25 biogeosciences.net/14/1825/2017/, 2017.

Faganeli, J. and Herndl, G.: Behaviour of Dissolved Organic Matter in Pore Waters of Near-Shore Marine Sediments, in: Diversity of Environmental Biogeochemistry, edited by Berthelin, J., vol. 6 of *Developments in Geochemistry*, pp. 157 – 170, Elsevier, https://doi.org/https://doi.org/10.1016/B978-0-444-88900-3.50020-5, http://www.sciencedirect.com/science/article/pii/B9780444889003500205, 1991.

30 Finke, N., Hoehler, T. M., and Jørgensen, B. B.: Hydrogen 'leakage' during methanogenesis from methanol and methylamine: implications for anaerobic carbon degradation pathways in aquatic sediments, Environmental Microbiology, 9, 1060–1071, https://doi.org/10.1111/j.1462-2920.2007.01248.x, https://onlinelibrary.wiley.com/doi/abs/10.1111/j.1462-2920.2007.01248.x, 2007.

Gibb, C. L. D. and Gibb, B. C.: Anion Binding to Hydrophobic Concavity Is Central to the Salting-in Effects of Hofmeister Chaotropes, Journal of the American Chemical Society, 133, 7344–7347, https://doi.org/10.1021/ja202308n, https://doi.org/10.1021/ja202308n, 2011.

35 Glock, N., Roy, A.-S., Romero, D., Wein, T., Weissenbach, J., Revsbech, N. P., Høgslund, S., Clemens, D., Sommer, S., and Dagan, T.: Metabolic preference of nitrate over oxygen as an electron acceptor in foraminifera from the Peruvian oxygen minimum zone, Proceedings of the National Academy of Sciences, 116, 2860–2865, https://doi.org/10.1073/pnas.1813887116, https://www.pnas.org/content/116/8/2860, 2019.

Gutiérrez, D., Sifeddine, A., Field, D. B., Ortlieb, L., Vargas, G., Chávez, F. P., Velazco, F., Ferreira, V., Tapia, P., Salvatteci, R., Boucher, H., Morales, M. C., Valdés, J., Reyss, J.-L., Campusano, A., Boussafir, M., Mandeng-Yogo, M., García, M., and Baumgartner, T.: Rapid reorganization in ocean biogeochemistry off Peru towards the end of the Little Ice Age, Biogeosciences, 6, 835–848, https://doi.org/10.5194/bg-6-835-2009, https://www.biogeosciences.net/6/835/2009/, 2009.

5 Hansen, H. and Koroleff, F.: Determination of nutrientss, chap. 10, pp. 159–228, John Wiley and Sons, 3 edn., https://doi.org/10.1002/9783527613984.ch10, 2007.

Hedges, J. I., Clark, W. A., and Come, G. L.: Fluxes and reactivities of organic matter in a coastal marine bay, Limnology and Oceanography, 33, 1137–1152, https://doi.org/10.4319/lo.1988.33.5.1137, https://aslopubs.onlinelibrary.wiley.com/doi/abs/10.4319/lo.1988.33.5.1137, 1988.

10 Heitmann, T. and Blodau, C.: Oxidation and incorporation of hydrogen sulfide by dissolved organic matter, Chemical Geology, 235, 12 – 20, https://doi.org/10.1016/j.chemgeo.2006.05.011, http://www.sciencedirect.com/science/article/pii/S0009254106002737, 2006.

Helms, J. R., Stubbins, A., Ritchie, J. D., Minor, E. C., Kieber, D. J., and Mopper, K.: Absorption spectral slopes and slope ratios as indicators of molecular weight, source, and photobleaching of chromophoric dissolved organic matter, Limnology and Oceanography, 53, 955–969, https://doi.org/10.4319/lo.2008.53.3.0955, https://aslopubs.onlinelibrary.wiley.com/doi/abs/10.4319/lo.2008.53.3.0955, 2008.

15 Holcombe, B. L., Keil, R. G., and Devol, A. H.: Determination of pore-water dissolved organic carbon fluxes from Mexican margin sediments, Limnology and Oceanography, 46, 298–308, https://doi.org/10.4319/lo.2001.46.2.0298, 2001.

Jørgensen, L., Stedmon, C. A., Kragh, T., Markager, S., Middelboe, M., and Søndergaard, M.: Global trends in the fluorescence characteristics and distribution of marine dissolved organic matter, Marine Chemistry, 126, 139 – 148, https://doi.org/https://doi.org/10.1016/j.marchem.2011.05.002, http://www.sciencedirect.com/science/article/pii/S0304420311000569, 2011.

Kalvelage, T., Lavik, G., Lam, P., Contreras, S., Arteaga, L., Löscher, C. R., Oschlies, A., Paulmier, A., Stramma, L., and Kuypers, M. M. M.: Nitrogen cycling driven by organic matter export in the South Pacific oxygen minimum zone, Nature Geoscience, 6, 228 EP –, https://doi.org/10.1038/ngeo1739, article, 2013.

Keeling, R. F., Körtzinger, A., and Gruber, N.: Ocean Deoxygenation in a Warming World, Annual Review of Marine Science, 2, 199–229, https://doi.org/10.1146/annurev.marine.010908.163855, https://doi.org/10.1146/annurev.marine.010908.163855, pMID: 21141663, 2010.

Komada, T., Reimers, C. E., Luther, G. W., and Burdige, D. J.: Factors affecting dissolved organic matter dynamics in mixed-redox to anoxic coastal sediments, Geochimica et Cosmochimica Acta, 68, 4099 – 4111, https://doi.org/10.1016/j.gca.2004.04.005, http://www.sciencedirect.com/science/article/pii/S0016703704002789, 2004.

Komada, T., Burdige, D. J., Crispo, S. M., Druffel, E. R., Griffin, S., Johnson, L., and Le, D.: Dissolved organic carbon dynamics in anaerobic sediments of the Santa Monica Basin, Geochimica et Cosmochimica Acta, 110, 253 – 273, https://doi.org/https://doi.org/10.1016/j.gca.2013.02.017, http://www.sciencedirect.com/science/article/pii/S0016703713001129, 2013.

Komada, T., Burdige, D. J., Li, H.-L., Magen, C., Chanton, J. P., and Cada, A. K.: Organic matter cycling across the sulfate-methane transition zone of the Santa Barbara Basin, California Borderland, Geochimica et Cosmochimica Acta, 176, 259 – 278, https://doi.org/10.1016/j.gca.2015.12.022, http://www.sciencedirect.com/science/article/pii/S0016703715007164, 2016.

35 Lalonde, K., Mucci, A., Ouellet, A., and Gélinas, Y.: Preservation of organic matter in sediments promoted by iron, Nature, 483, 198–200, https://doi.org/10.1038/nature10855, https://doi.org/10.1038/nature10855, 2012.

Lavery, P. S., Oldham, C. E., and Ghisalberti, M.: The use of Fick's First Law for predicting porewater nutrient fluxes under diffusive conditions, Hydrological Processes, 15, 2435–2451, https://doi.org/10.1002/hyp.297, https://onlinelibrary.wiley.com/doi/abs/10.1002/hyp.297, 2001.

Le Moigne, F. A. C., Cisternas-Novoa, C., Piontek, J., Maßmig, M., and Engel, A.: On the effect of low oxygen concentrations on bacterial degradation of sinking particles, Scientific Reports, 7, 16 722, https://doi.org/10.1038/s41598-017-16903-3, https://doi.org/10.1038/s41598-017-16903-3, 2017.

Liu, K.-K. and Kaplan, I. R.: Denitrification rates and availability of organic matter in marine environments, Earth and Planetary Science Letters, 68, 88 – 100, https://doi.org/https://doi.org/10.1016/0012-821X(84)90142-0, http://www.sciencedirect.com/science/article/pii/0012821X84901420, 1984.

Liu, Z. and Lee, C.: The role of organic matter in the sorption capacity of marine sediments, Marine Chemistry, 105, 240 – 257, https://doi.org/https://doi.org/10.1016/j.marchem.2007.02.006, http://www.sciencedirect.com/science/article/pii/S0304420307000527, 2007.

Loginova, A. N., Thomsen, S., and Engel, A.: Chromophoric and fluorescent dissolved organic matter in and above the oxygen minimum zone off Peru, Journal of Geophysical Research: Oceans, 121, 7973–7990, https://doi.org/10.1002/2016JC011906, https://agupubs.onlinelibrary.wiley.com/doi/abs/10.1002/2016JC011906, 2016.

Loginova, A. N., Thomsen, S., Dengler, M., Lüdke, J., and Engel, A.: Diapycnal dissolved organic matter supply into the upper Peruvian oxycline, Biogeosciences, 16, 2033–2047, https://doi.org/10.5194/bg-16-2033-2019, https://www.biogeosciences.net/16/2033/2019/, 2019.

Lüdke, J., Dengler, M., Sommer, S., Clemens, D., Thomsen, S., Krahmann, G., Dale, A. W., Achterberg, E. P., and Visbeck, M.: Influence of intraseasonal eastern boundary circulation variability on hydrography and biogeochemistry off Peru, Ocean Science Discussions, 2019, 1–31, https://doi.org/10.5194/os-2019-93, https://www.ocean-sci-discuss.net/os-2019-93/, 2019.

Ludwig, W., Probst, J.-L., and Kempe, S.: Predicting the oceanic input of organic carbon by continental erosion, Global Biogeochemical Cycles, 10, 23–41, https://doi.org/10.1029/95GB02925, https://agupubs.onlinelibrary.wiley.com/doi/abs/10.1029/95GB02925, 1996.

Marsay, C. M., Sanders, R. J., Henson, S. A., Pabortsava, K., Achterberg, E. P., and Lampitt, R. S.: Attenuation of sinking particulate organic carbon flux through the mesopelagic ocean, Proceedings of the National Academy of Sciences, 112, 1089–1094, https://doi.org/10.1073/pnas.1415311112, https://www.pnas.org/content/112/4/1089, 2015.

Martin, W. R. and McCorkle, D. C.: Dissolved organic carbon concentrations in marine pore waters determined by high-temperature oxidation, Limnology and Oceanography, 38, 1464–1479, https://doi.org/10.4319/lo.1993.38.7.1464, https://aslopubs.onlinelibrary.wiley.com/doi/abs/10.4319/lo.1993.38.7.1464, 1993.

Maßmig, M., Piontek, J., Le Moigne, F., Cisternas-Novoa, C., and Engel, A.: Potential role of oxygen and inorganic nutrients on microbial carbon turnover in the Baltic Sea, Aquatic Microbial Ecology, 83, 95–108, https://doi.org/10.3354/ame01902, https://www.int-res.com/abstracts/ame/v83/n1/p95-108/, 2019.

Maßmig, M., Lüdke, J., Krahmann, G., and Engel, A.: Bacterial degradation activity in the eastern tropical South Pacific oxygen minimum zone, Biogeosciences, 17, 215–230, https://doi.org/10.5194/bg-17-215-2020, https://www.biogeosciences.net/17/215/2020/, 2020.

Moran, M. A. and Zepp, R. G.: Role of photoreactions in the formation of biologically labile compounds from dissolved organic matter, Limnology and Oceanography, 42, 1307–1316, https://doi.org/10.4319/lo.1997.42.6.1307, https://aslopubs.onlinelibrary.wiley.com/doi/abs/10.4319/lo.1997.42.6.1307, 1997.

Mosch, T., Sommer, S., Dengler, M., Noffke, A., Bohlen, L., Pfannkuche, O., Liebetrau, V., and Wallmann, K.: Factors influencing the distribution of epibenthic megafauna across the Peruvian oxygen minimum zone, Deep Sea Research Part I: Oceanographic Re-

search Papers, 68, 123 – 135, https://doi.org/https://doi.org/10.1016/j.dsr.2012.04.014, http://www.sciencedirect.com/science/article/pii/ S0967063712001410, 2012.

Murphy, K. R., Stedmon, C. A., Graeber, D., and Bro, R.: Fluorescence spectroscopy and multi-way techniques. PARAFAC, Anal. Methods, 5, 6557–6566, https://doi.org/10.1039/C3AY41160E, http://dx.doi.org/10.1039/C3AY41160E, 2013.

5   Murphy, K. R., Stedmon, C. A., Wenig, P., and Bro, R.: OpenFluor– an online spectral library of auto-fluorescence by organic compounds in the environment, Anal. Methods, 6, 658–661, https://doi.org/10.1039/C3AY41935E, 10.1039/C3AY41935E, 2014.

Nelson, N. B. and Siegel, D. A.: The Global Distribution and Dynamics of Chromophoric Dissolved Organic Matter, Annual Review of Marine Science, 5, 447–476, https://doi.org/10.1146/annurev-marine-120710-100751, https://doi.org/10.1146/ annurev-marine-120710-100751, pMID: 22809178, 2013.

10   Pantoja, S., Rossel, P., Castro, R., Cuevas, L. A., Daneri, G., and Córdova, C.: Microbial degradation rates of small peptides and amino acids in the oxygen minimum zone of Chilean coastal waters, Deep Sea Research Part II: Topical Studies in Oceanography, 56, 1055 – 1062, https://doi.org/10.1016/j.dsr2.2008.09.007, http://www.sciencedirect.com/science/article/pii/S0967064508003251, the Oceanography of the Eastern South Pacific II: The Oxygen Minimum Zone, 2009.

Pennington, J. T., Mahoney, K. L., Kuwahara, V. S., Kolber, D. D., Calienes, R., and Chavez, F. P.: Primary production in the eastern tropical
15   Pacific: A review, Progress in Oceanography, 69, 285 – 317, https://doi.org/10.1016/j.pocean.2006.03.012, http://www.sciencedirect.com/ science/article/pii/S0079661106000358, a Review of Eastern Tropical Pacific Oceanography, 2006.

Prokopenko, M., Sigman, D., Berelson, W., Hammond, D., Barnett, B., Chong, L., and Townsend-Small, A.: Denitrification in anoxic sediments supported by biological nitrate transport, Geochimica et Cosmochimica Acta, 75, 7180 – 7199, https://doi.org/10.1016/j.gca.2011.09.023, http://www.sciencedirect.com/science/article/pii/S0016703711005448, 2011.

20   Rodríguez-Morata, C., Díaz, H. F., Ballesteros-Canovas, J. A., Rohrer, M., and Stoffel, M.: The anomalous 2017 coastal El Niño event in Peru, Climate Dynamics, 52, 5605–5622, https://doi.org/10.1007/s00382-018-4466-y, https://doi.org/10.1007/s00382-018-4466-y, 2019.

Schunck, H., Lavik, G., Desai, D. K., Großkopf, T., Kalvelage, T., Löscher, C. R., Paulmier, A., Contreras, S., Siegel, H., Holtappels, M., Rosenstiel, P., Schilhabel, M. B., Graco, M., Schmitz, R. A., Kuypers, M. M. M., and LaRoche, J.: Giant Hydrogen Sulfide Plume in the Oxygen Minimum Zone off Peru Supports Chemolithoautotrophy, PLOS ONE, 8, 1–18, https://doi.org/10.1371/journal.pone.0068661,
25   https://doi.org/10.1371/journal.pone.0068661, 2013.

Seiter, K., Hensen, C., Schröter, J., and Zabel, M.: Organic carbon content in surface sediments—defining regional provinces, Deep Sea Research Part I: Oceanographic Research Papers, 51, 2001 – 2026, https://doi.org/10.1016/j.dsr.2004.06.014, http://www.sciencedirect. com/science/article/pii/S0967063704001384, 2004.

Smith, D. C., Simon, M., Alldredge, A. L., and Azam, F.: Intense hydrolytic enzyme activity on marine aggregates and implications for rapid
30   particle dissolution, Nature, 359, 139–142, https://doi.org/10.1038/359139a0, https://doi.org/10.1038/359139a0, 1992.

Sommer, S., Türk, M., Kriwanek, S., and Pfannkuche, O.: Gas exchange system for extended in situ benthic chamber flux measurements under controlled oxygen conditions: First application—Sea bed methane emission measurements at Captain Arutyunov mud volcano, Limnology and Oceanography: Methods, 6, 23–33, https://doi.org/10.4319/lom.2008.6.23, https://aslopubs.onlinelibrary.wiley.com/doi/ abs/10.4319/lom.2008.6.23, 2008.

35   Sommer, S., Gier, J., Treude, T., Lomnitz, U., Dengler, M., Cardich, J., and Dale, A.: Depletion of oxygen, nitrate and nitrite in the Peruvian oxygen minimum zone cause an imbalance of benthic nitrogen fluxes, Deep Sea Research Part I: Oceanographic Research Papers, 112, 113 – 122, https://doi.org/10.1016/j.dsr.2016.03.001, http://www.sciencedirect.com/science/article/pii/S0967063715300819, 2016.

Stedmon, C. A. and Bro, R.: Characterizing dissolved organic matter fluorescence with parallel factor analysis: a tutorial, Limnology and Oceanography: Methods, 6, 572–579, https://doi.org/10.4319/lom.2008.6.572, https://aslopubs.onlinelibrary.wiley.com/doi/abs/10.4319/lom.2008.6.572, 2008.

Stramma, L., Hüttl, S., and Schafstall, J.: Water masses and currents in the upper tropical northeast Atlantic off northwest Africa, Journal of Geophysical Research: Oceans, 110, https://doi.org/10.1029/2005JC002939, https://agupubs.onlinelibrary.wiley.com/doi/abs/10.1029/2005JC002939, 2005.

Stramma, L., Johnson, G. C., Sprintall, J., and Mohrholz, V.: Expanding Oxygen-Minimum Zones in the Tropical Oceans, Science, 320, 655–658, https://doi.org/10.1126/science.1153847, https://science.sciencemag.org/content/320/5876/655, 2008.

Sutton, R. and Sposito, G.: Molecular Structure in Soil Humic Substances: The New View, Environmental Science & Technology, 39, 9009–9015, https://doi.org/10.1021/es050778q, https://doi.org/10.1021/es050778q, 2005.

Szewzyk, U., Szewzyk, R., and Schink, B.: Methanogenic degradation of hydroquinone and catechol via reductive dehydroxylation to phenol, FEMS Microbiology Letters, 31, 79 – 87, https://doi.org/10.1016/0378-1097(85)90003-5, http://www.sciencedirect.com/science/article/pii/0378109785900035, 1985.

Thomsen, S., Kanzow, T., Krahmann, G., Greatbatch, R. J., Dengler, M., and Lavik, G.: The formation of a subsurface anticyclonic eddy in the Peru-Chile Undercurrent and its impact on the near-coastal salinity, oxygen, and nutrient distributions, Journal of Geophysical Research: Oceans, 121, 476–501, https://doi.org/10.1002/2015JC010878, https://agupubs.onlinelibrary.wiley.com/doi/abs/10.1002/2015JC010878, 2016.

Tomaszewski, J. E., Schwarzenbach, R. P., and Sander, M.: Protein Encapsulation by Humic Substances, Environmental Science & Technology, 45, 6003–6010, https://doi.org/10.1021/es200663h, https://doi.org/10.1021/es200663h, 2011.

Ullman, W. J. and Aller, R. C.: Diffusion coefficients in nearshore marine sediments1, Limnology and Oceanography, 27, 552–556, https://doi.org/10.4319/lo.1982.27.3.0552, https://aslopubs.onlinelibrary.wiley.com/doi/abs/10.4319/lo.1982.27.3.0552, 1982.

Westerhoff, P. and Mash, H.: Dissolved organic nitrogen in drinking water supplies: a review, Journal of Water Supply: Research and Technology-Aqua, 51, 415–448, https://doi.org/10.2166/aqua.2002.0038, https://doi.org/10.2166/aqua.2002.0038, 2002.

Wolf, F. T. and Stevens, M. V.: THE FLUORESCENCE OF CAROTENOIDS, Photochemistry and Photobiology, 6, 597–599, https://doi.org/10.1111/j.1751-1097.1967.tb08761.x, https://onlinelibrary.wiley.com/doi/abs/10.1111/j.1751-1097.1967.tb08761.x, 1967.

Yang, L., Choi, J. H., and Hur, J.: Benthic flux of dissolved organic matter from lake sediment at different redox conditions and the possible effects of biogeochemical processes, Water Research, 61, 97 – 107, https://doi.org/https://doi.org/10.1016/j.watres.2014.05.009, http://www.sciencedirect.com/science/article/pii/S0043135414003546, 2014.

Zsolnay, A., Baigar, E., Jimenez, M., Steinweg, B., and Saccomandi, F.: Differentiating with fluorescence spectroscopy the sources of dissolved organic matter in soils subjected to drying, Chemosphere, 38, 45 – 50, https://doi.org/https://doi.org/10.1016/S0045-6535(98)00166-0, http://www.sciencedirect.com/science/article/pii/S0045653598001660, 1999.
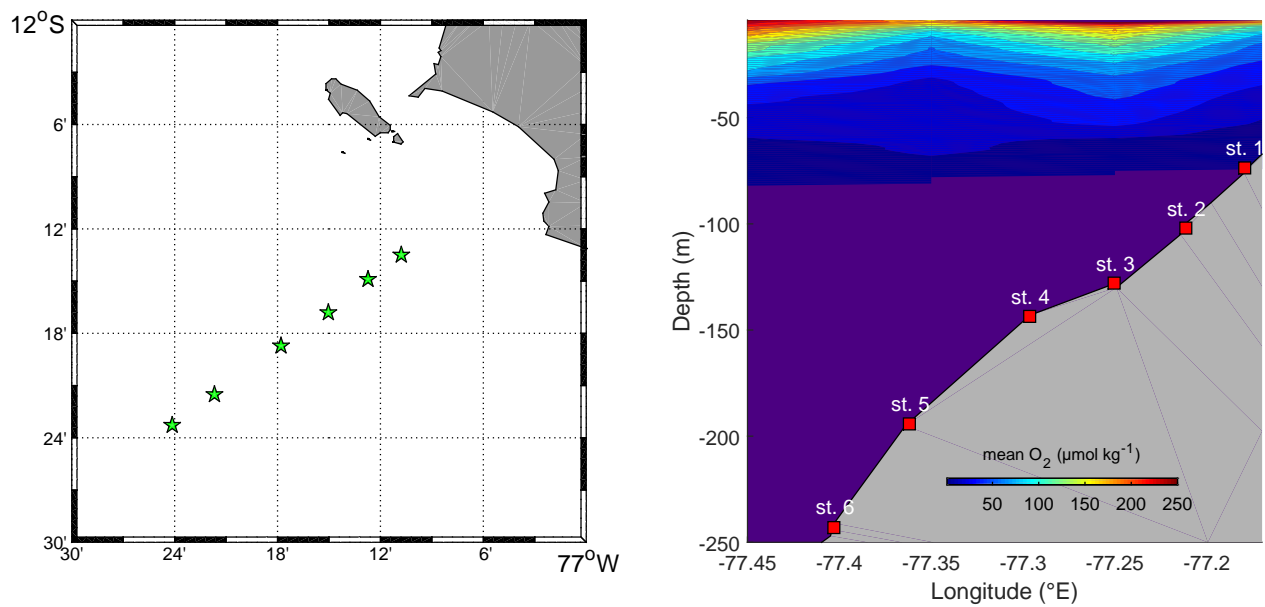
Figure 1. Distribution of sampling stations. Right: mean oxygen plot (the O_2 values were averaged over 1m depth and 0.1^o longitude intervals). The indigo colour represents values below 1 μmol kg^{-1}
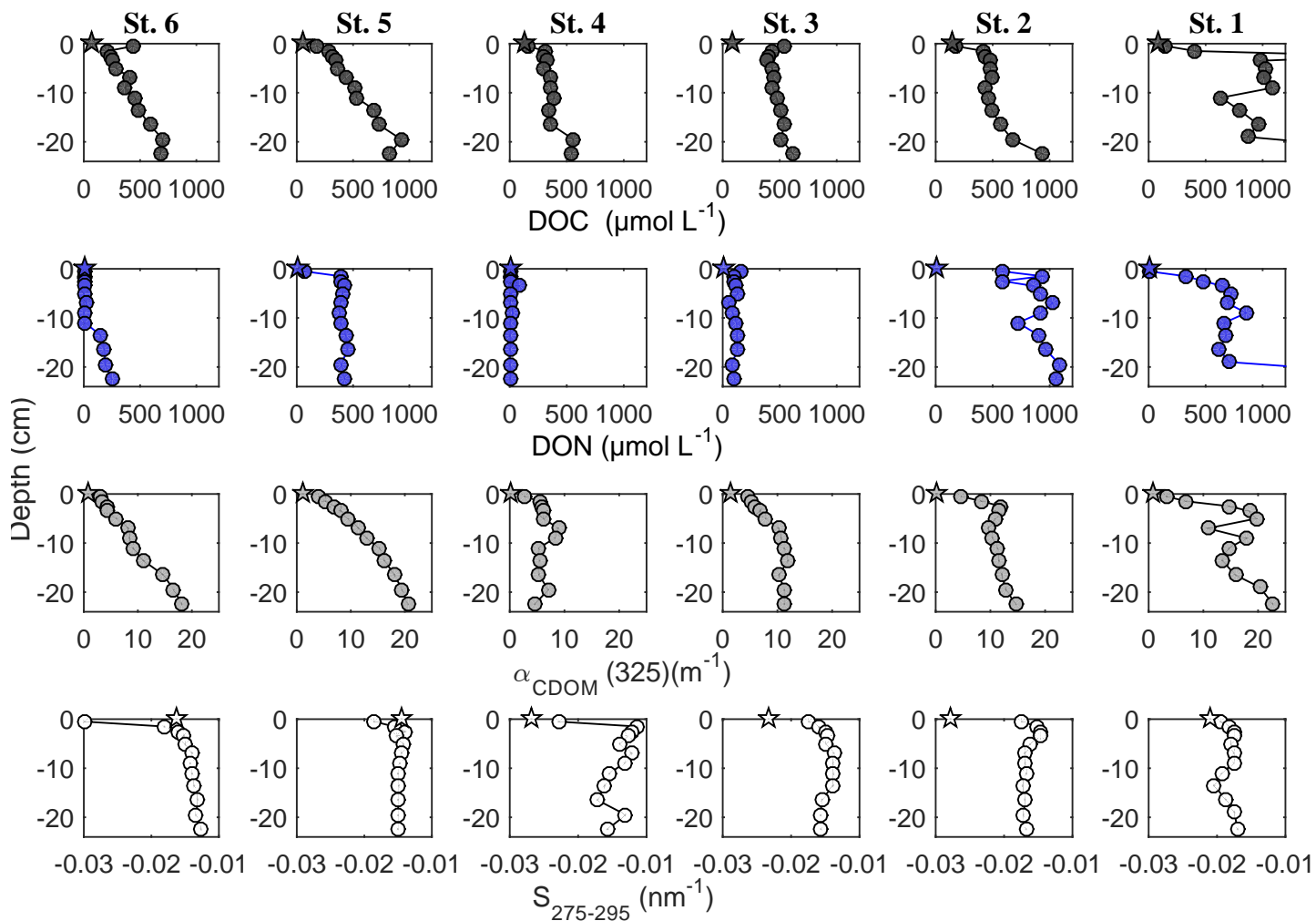
Figure 2. Porewater DOC (dark grey symbols), DON (blue symbols), $a_{CDOM}(325)$ (light grey symbols) and $S_{275-295}$ (white symbols) distribution within the sediments: depth profiles. Circles represent concentration/value, measured in the porewater sample, pentagrams represent the initial concentration/value of the bottom water.
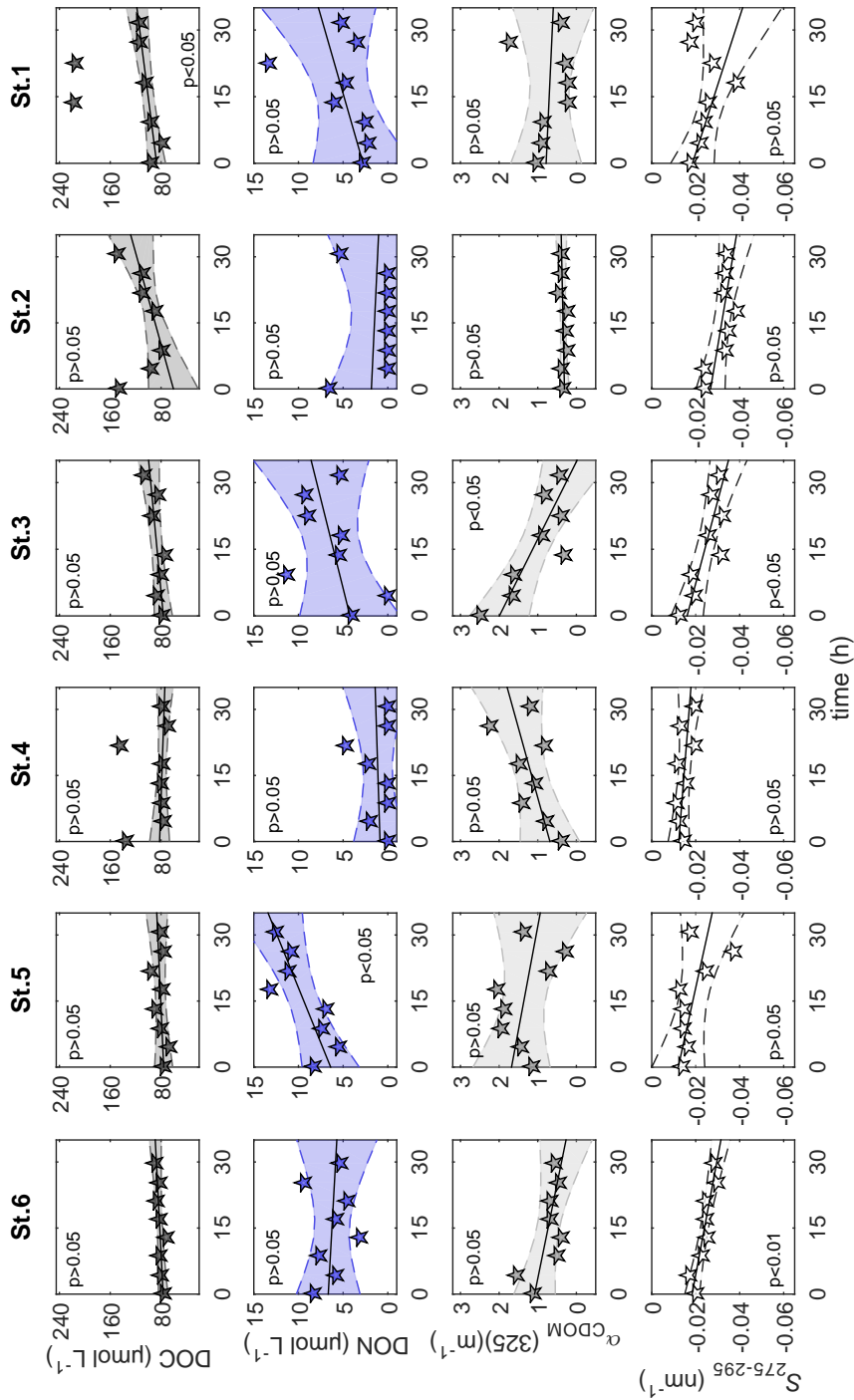
Figure 3. Distribution of DOC and CDOM parameters, $a_{CDOM}(325)$ and $S_{275-295}$, measured in BIGO chambers over time. Polynomial fit (1st order) was used for linear regression analyses: t_0 and data included in brackets were excluded from the analyses.
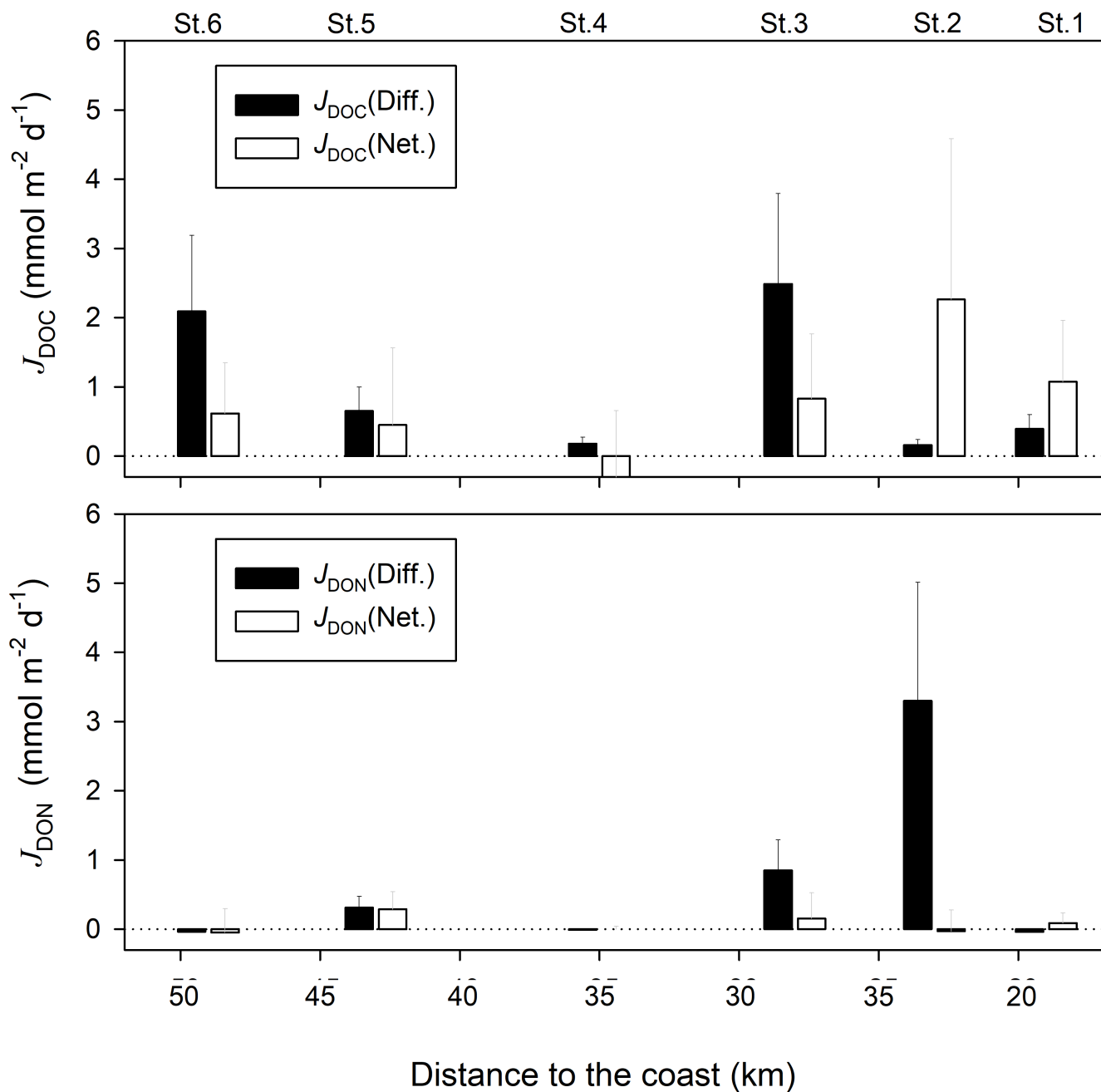
Figure 4. Diffusive and *in situ* net DOC (upper panel) and DON (lower panel) fluxes, evaluated at 12°S transect during this study.
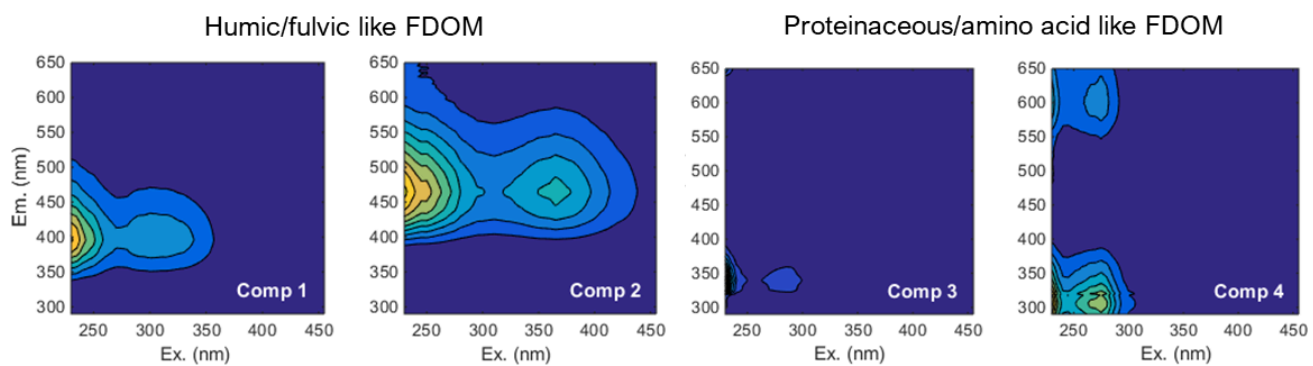
Figure 5. Four-components, which were found and validated by PARAFAC analyses after Murphy et al.(2013)
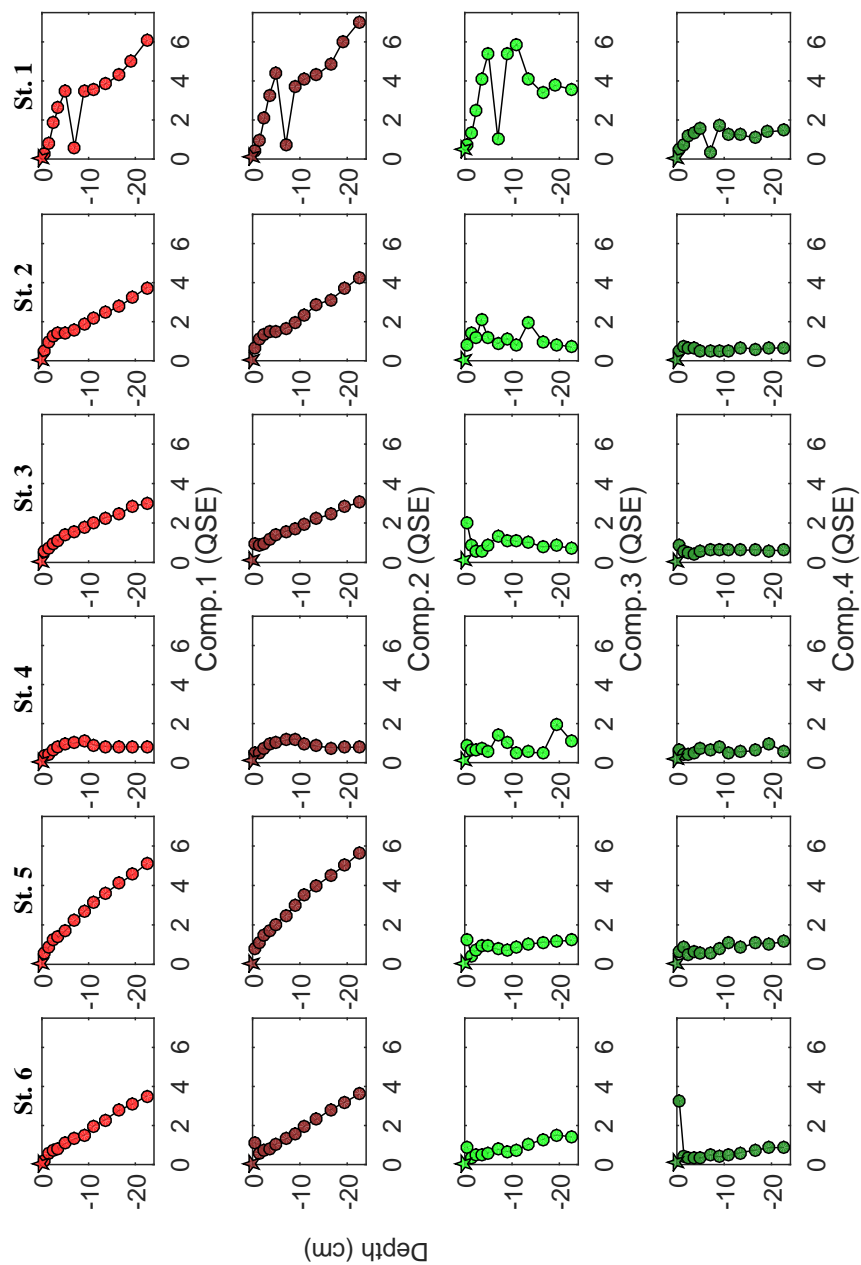
Figure 6. Porewater FDOM components distribution within the sediments: depth profiles. Humic-like Comp.1 and Comp.2 represented by light and dark red symbols, respectively. Amino acid-like Comp.3 and Comp.4 represented by light and dark green symbols, respectively. Circles represent concentration/value, measured in the porewater sample, pentagrams represent the initial concentration/value of the bottom water.
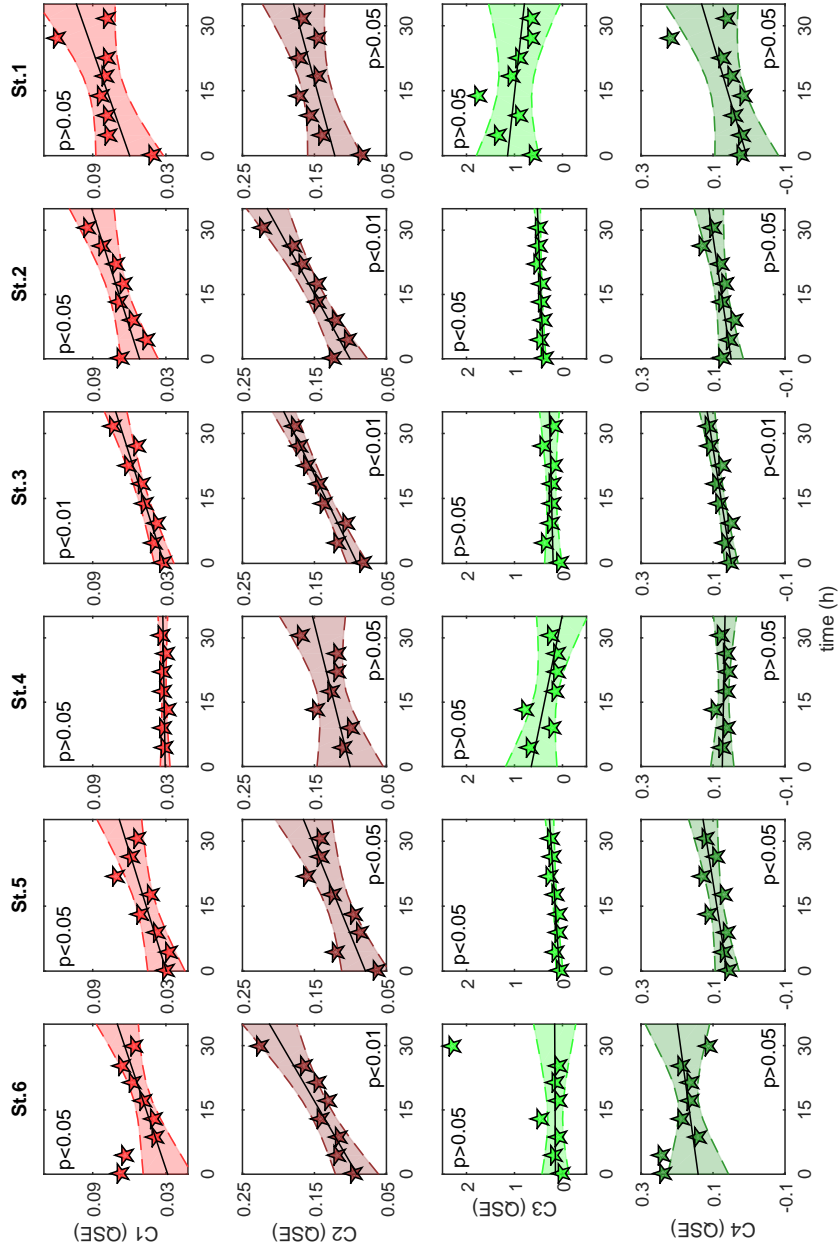
Figure 7. Distribution of FDOM components, measured in BIGO chambers over time. Polynomial fit (1st order) was used for linear regression analyses: t_0 and data included in brackets were excluded from the analyses.
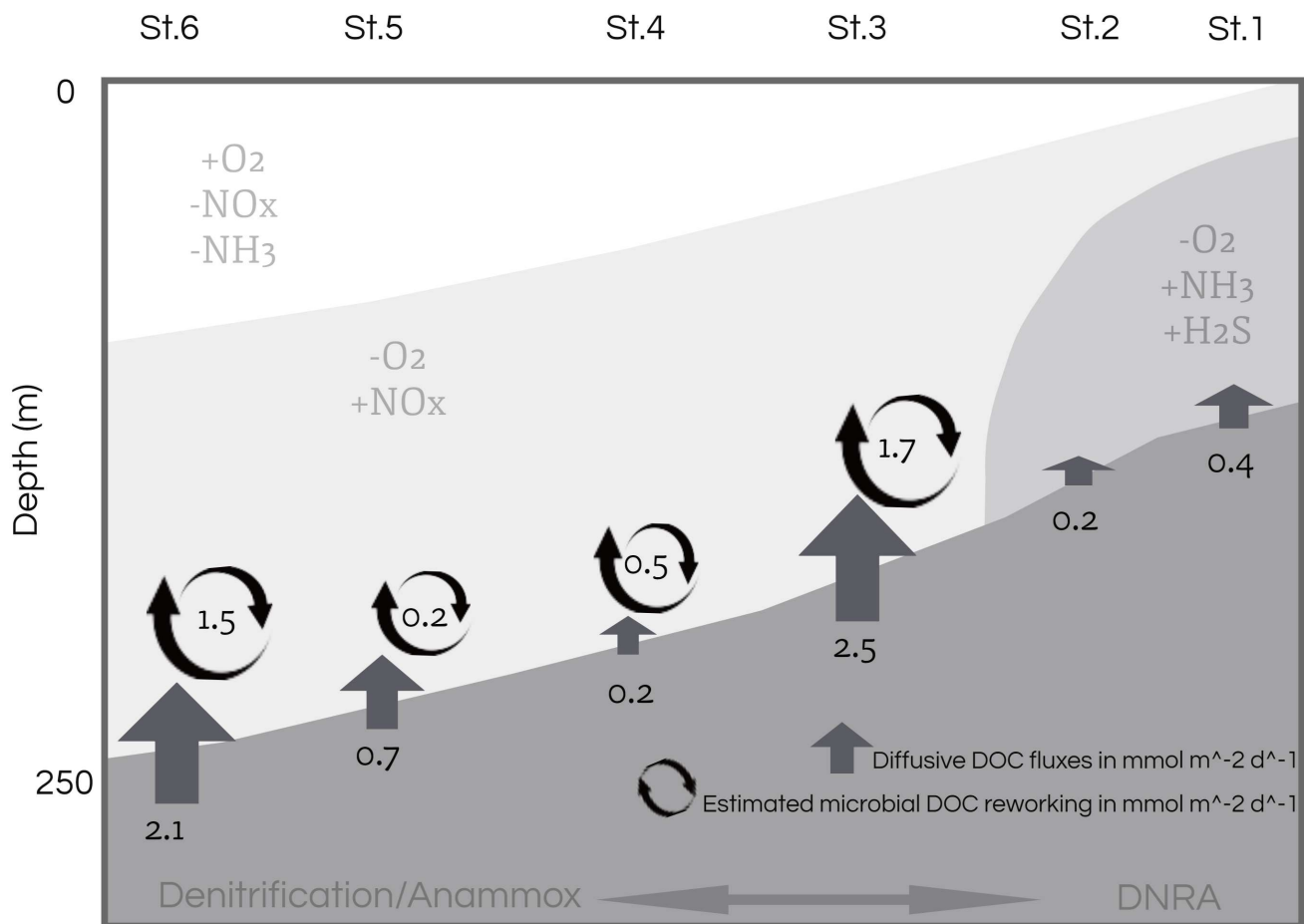
Figure 8. Conceptual view of DOM cycling near the sediment off Peru. Arrows directed out of the sediment represent diffusive fluxes of DOC ($J_{DOC}(Diff.)$) in $\mathrm{mmol\,m^{-2}d^{-1}}$. Circular arrows indicate microbial DOM reworking, calculated as a difference of $J_{DOC}(Diff.)$ and net *in situ* flux ($J_{DOC}(Net)$) at each station.

Table 1. Stations and instruments deployed during our study on the Peruvian margin.

Station	BIGO	MUC	Date (BIGO)	Date (MUC)	Latitude (°N)	Longitude (°E)	Depth (m)	Temp. (°C)	Porosity	O_2 (μmol kg^{-1})	Dale et al. (2015)
St.1	533 BIGO II-IV	483 MUC 8	27 Apr	24 Apr	-77.180	-12.225	74	16.2	0.93	b.d.	Middle
St.2	642 BIGO II-II	577 MUC 11	09 May	01 May*	-77.212	-12.248	102	15.9	0.96	11	Shelf
St.3	488 BIGO II-III	426 MUC 6	24 Apr	19 Apr	-77.250	-12.280	128	15.2	0.95	b.d.	Outer
St.4	503 BIGO I-III	651 MUC8	25 Apr	10 May	-77.297	-12.312	144	14.6	0.94	b.d.	Shelf
St.5	471 BIGO I-II	692 MUC 15	23 Apr	13 May	-77.362	-12.358	194	13.9	0.95	b.d.	
St.6	415 BIGO II-I	412 MUC 5	18 Apr	18 Apr	-77.403	-12.388	243	12.9	0.95	b.d.	Continental Slope

* NH_4^+ concentrations were measured at 787MUC33 on 20th of May at -12.247°N and -77.212°E.

Station depth was recorded from the ship winch. Bottom water temperature and O_2 are recorded by CTD. "b.d." stands for "below detection". Detection limit of O_2 is 5 μmol kg^{-1} (Dale et al., 2015). Porosity is given for the upper 0.5 cm.